Alma Mater Studiorum - Università di Bologna

DOTTORATO DI RICERCA IN ONCOLOGIA, EMATOLOGIA E PATOLOGIA

Ciclo 33

**Settore Concorsuale:** 06/G1

**Settore Scientifico Disciplinare:** MED/38

# Study of pathway alterations in Gaucher disease by induced pluripotent stem cell models

**Presentata da:** Daria Messelodi

**Coordinatore Dottorato**
Prof. Manuela Ferracin

**Supervisore**
Prof. Andrea Pession

**Co-supervisore**
Dott.ssa Annalisa Astolfi

Esame finale anno 2021

# Contents

# Abstract

Gaucher disease (GD) is a lysosomal storage disorder characterized by $\beta$-glucocerebrosidase enzyme deficiency, due to mutations in the *GBA1* gene. Typical features of the disease are the unrestrained activation of the inflammatory response and a massive neuronal cell death in the neuronopathic forms, whose molecular pathways are still unclear. GD patients, even if affected by a monogenic disease, exhibit a wide range of symptoms, ranging from very mild hematological and visceral phenotypes, to severe neurological involvement. The absence of a clear genotype-phenotype correlation supports the idea that other players act together with *GBA1* mutations to give rise to the final clinical picture.

To identify new pathway alterations occurring in the pathological condition, GD patient-derived induced pluripotent stem cell (iPSC) lines have been generated, characterized and isogenic gene corrected in the mutation site. iPSC differentiation towards the macrophage fate has been employed to investigate the hematopoietic compartment where the differentiation and growth potential of the cells was evaluated. While GD iPSCs are able to efficiently give rise to CD43+/CD45+ progenitors and mature CD14+/CD163+ monocyte/macrophages, they showed a decreased proliferative potential compared to healthy donor cells, either in semisolid and liquid culture, exhibiting a growth impairment. The activation of necroptosis pathway, a regulated cell death mechanism induced by inflammation, emerged in both pluripotent and differentiated GD cells, that showed a significant upregulation of two of the main effectors, RIPK3 and MLKL. To dissect brain inflammatory mechanisms, iPSC have been differentiated to neural precursor cells (NPC) and dopaminergic neurons. GD cells presented also at the NPC state both a growth deficit and an increased cell death rate. Since the Hippo pathway is involved in the control of many cellular mechanisms as proliferation, differentiation and cell death and was recently reported as hyper activated in many neurodegenerative disorders, we evaluated its activation in GD lines. Interestingly, many of the pathway transcriptional targets were downregulated in GD neurons and the cellular localization of YAP, the main pathway effector, resulted less nuclear, suggesting that the Hippo pathway core is highly activated in the pathogenic context.

The identification of altered signaling pathways, like necroptosis and Hippo, that may contribute to the cellular metabolism imbalance, are instrumental in the development of new pharmacological approaches to GD that are especially required for neuronopathic patients.

# 1 Introduction

## 1.1 Gaucher disease

Gaucher disease (GD) is known as the most common lysosomal storage disorder. It is a genetic disease with autosomic recessive heritability. The causative genetic alteration involves the *GBA1* gene, encoding for ß-glucocerebrosidase (GCase), a lysosomal enzyme responsible for the glucosylceramide (GluCer) degradation. The first description of GD was done by Philippe Gaucher in 1882 reporting a patient with a non leukemic related marked splenomegaly, while the recognition of the causative enzymatic defect and the characterization of the involved protein and gene was achieved thanks to the work of Roscoe Brady in 1960s[1]. Nowadays the incidence is between 1/40000 and 1/60000 in the general population, with the exception of the Ashkenazi Jewish where it can reach 1/800[2].

### 1.1.1 Physiopathology

GCase catalyses the hydrolysis of GluCer into ceramide and glucose, playing a crucial role in the degradation of complex lipids and in the cell membrane turnover. Mutations into *GBA1* gene lead to GCase structure modifications that have important effects on the enzyme activity. Some milder mutations result in the protein misfolding causing a strong activity reduction, others can generate a complete lack of functionality. The loss of GCase hydrolytic function causes the accumulation of GluCer (the enzyme direct substrate) and glucosylsphingosine (GlcSph - the deacylated form of GluCer) in the lysosomes and cytoplasm of the affected cells[3] (Figure 1). The substrates accumulation primarily regards reticulo-endothelial system cells, as monocytes and macrophages, playing a role in the degradation of cells containing high amount of glycosphingolipids like erythrocytes and leukocytes[4]. Gaucher macrophages switch to an enlarged shape, the cytoplasm is filled with fibrillar material[5] and, because of their ability to massively infiltrate spleen, liver and bone narrow, they are considered as the main cause of the disease symptomatology. However, many disorder features suggest that this macrophage-centric view is not enough to explain the complex clinical picture of many GD cases that sometimes include also malignancy, autoimmune disease, Parkinson disease and osteoporosis, linked to multiple cell types and pathways[6]. The sphingolipids accumulation occurs in some cases also in the neuronal lineage, causing severe neuronal loss, astrocytosis and microglial proliferation[7,8]. Little is known about the molecular events lead-

ing to neuronal death especially because the GluCer accumulation in neurons is significant only when residual GCase activity is strongly impaired by the most severe *GBA1* mutations[9]. However, elevated levels of GlcSph have been found in the cerebral and cerebellar cortices of neuronopathic GD patients[9] and, considering that this molecule has already been identified as a potential neurotoxin[10], it can be involved in the developing of neurological signs.

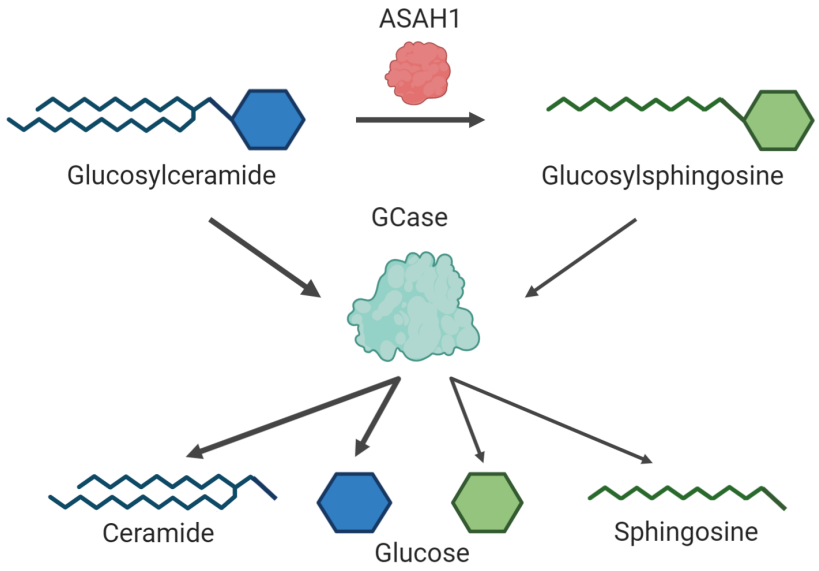


Figure 1: **GCase role in glicosphingolips degradation.** The enzyme is able to hydrolyse GluCer and, in a smaller amount, also GlcSph (probably obtained from the removal of an acetyl group from GluCer by the acid ceramidase ASAH1 enzyme activity).

### 1.1.2 Genetics

*GBA1* has been identified as the gene encoding for GCase[11]. It is located on chromosome 1 (1q21), 16 kb upstream of its highly homologous pseudogene *GBAP*. *GBA1* has a 7.6 kb sequence, made of 11 exons and 10 introns (Figure 2). The sequence identity between *GBA1* and *GBAP* is equal to 96% and the gene structure is exactly the same[12]. *GBA1* cDNA is almost 2 kb and two different in-frame translational start site are present in exon 1 and 2 giving rise to two polypeptides with different size signal peptide, both processed to the 497-residue mature enzyme. Tissue levels of GBA mRNA is variable among different cell types and they seem not to be correlated with the enzymatic activity[12].

More than 400 *GBA1* variants associated with GD manifestations have been identified[13]. Point mutations, small insertion and deletions, splice junctions and recombination events

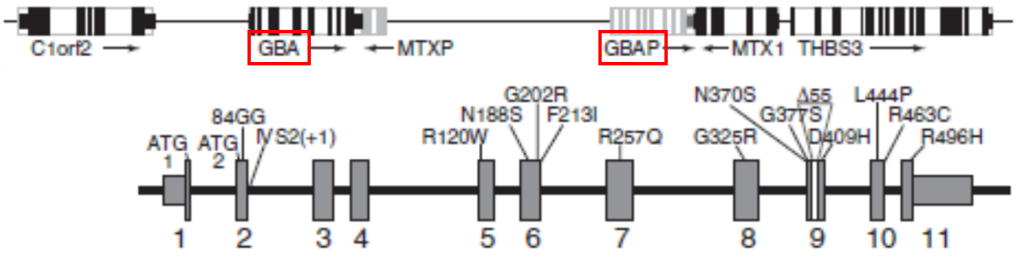


Figure 2: ***GBA1* gene structure and mutations.** Modified from Hruska et al. 2008[12].

with the pseudogene, resulting from gene conversion, fusion or duplication, have been reported[12]. The first two identified mutations are c.1226A < G (N370S) and c.1448T > C (L444P), which are still the most frequently found in the european population. Different variants are indeed more represented in different ethnic groups. N370S is the most common mutation among Ashkenazi Jew patients, as well as c.115 + 1G > A (IVS2 + 1), c.1504C > T (R463C), and c.1604G > A (R496H), which are are commonly found in GD type 1 patients. In Asia, where the neuropathic forms of GD are more frequent, the c.1448T > C (L444P) and the c.754T > A (F252I) mutations, usually associated with GD type 2 and 3, are more frequent. L444P is also the most recurrent mutation among Caucasians with a non-Ashkenazi Jew ancestry[14]. Even if the knowledge of *GBA1* mutations spectrum mutation is increasing, it is still very difficult to correlate genotypic data with phenotypic manifestations. The severity of a specific mutation is very hard to predict, especially because the final clinical picture is driven by the combined effect of both mutated alleles. The mutations distribution differs significantly in patients with neuronopathic GD; type 2 patients frequently present recombinant and rare alleles[15], while point mutations as c.1448T4C (L444P) and c.1504C4T (R463C) are common in the visceral forms of GD type 3. C.680A4G (N188S), c.1246G4A (G377S) and c.1297G4T (V394L) combined with a null or recombinant allele are characteristic of patients with myoclonic epilepsy. The point mutation c.1342G4C (D409 H) is usually correlated with cardiac involvement and hydrocephalus[12]. Despite these associations, for many patients a clear genotype-phenotype correlation remains very difficult to asses. The hypothesis that other factors acting along with *GBA1* mutations to drive the final clinical picture, is commonly shared. Many studies are nowadays focusing on the role of potential modifier genes, interacting pathways and external environmental factors[16].

GD is considered a monogenic disorder even if there are some reported *GBA1* wild type patients with clear GD characteristics and symptomatology carrying mutation in other *GBA1*

related genes as *SCARB2* and *PSAP*. SCARB2 encodes for the membrane protein LIMP2, that regulates lysosomal/endosomal transport and is involved in GCase lysosomal import [17]. Prosaposin C, encoded by the *PSAP* gene, is an essential activator of GCase and a cofactor of many lysosomal hydrolysis processes [18].

### 1.1.3 Clinical manifestations

GD is characterized by a wide spectrum of clinical manifestations, with a phenotypic variability that is evident also in patients carrying the same *GBA1* mutation; while some of them display only mild systemic symptoms with visceral involvement, others are affected by a severe neurological form [16]. The commonly used clinical classification divides patients into three groups depending on the neuronal involvement degree.

GD type 1 is the most prevalent disease form, it is characterized by visceral, hematologic and skeletal manifestations. Patients generally show hepatosplenomegaly with abdominal distention. The accumulation of Gaucher cells in the bone marrow together with hypersplenism results in cytopenia. Anemia and thrombocytopenia indeed are the most common hematological signs in symptomatic GD patients [19]. Additional manifestations include leukopenia, acquired coagulopathy, vitamin B12 deficiency and hyperferritinemia. Bone involvement in GD primary regards the bone marrow compartment, which functionality and structure are impaired because of Gaucher cells infiltration leading to inflammation, impaired hematopoiesis and fibrosis. Moreover, the engagement of osteoblast and endothelial cells contributes in the manifestations of avascular osteonecrosis and osteopenia and, in the worst cases, acute bone crisis [20]. Even if there is no primary neurological involvement, type 1 GD patients have a higher probability to develop peripheral neuropathy and Parkinson disease (PD). The link between GBA and PD is still unclear but it is known that gene mutations confer a risk for PD onset in the biallelic form as well as in the heterozygote carrier state. [21]. Also cancer is a condition that occurs more frequently in GD type 1 patients than in the general population; especially multiple myeloma and non-myeloma hematological malignancies, but also hepatocellular and renal cell carcinoma are frequently reported [20].

Type 2 is the most severe form of the disease, it is accompanied by severe neurological symptoms that can occur either prenatally or in the first months of life. The disease has a rapid progress and is followed by death within the first years of life. Hydrops fetalis is recurrent in the perinatal lethal cases. Newborns usually present skin abnormalities, hep-

atosplenomegaly and neurological signs as arthrogyphosis, microcephaly or hypokinesia[22]. Type 3 GD form is characterized by less severe neurological signs, that appear later in life and have a slower progression. Cognitive impairment, horizontal supranuclear gaze palsy, saccadic eye movement abnormalities, muscle weakness, ataxia and progressive myoclonic epilepsy are among the most common symptoms. Some patients also present visceral involvement, including hepatosplenomegaly, anemia and bone manifestations. A particular genotype (D409H homozygosis) is associated with corneal opacity and heart disease with progressive valvular calcification[23].

It is estimated that approximately 1% of Gaucher patients carry type 2 disease, and 5% have the type 3.

The distinctions between GD type 2 and 3 are related to the degree of progressivity and age at onset of neurological involvement, with type 2 having a more severe clinical course[24]. Although this classification has a clinical utility, GD manifestations tend to represent a phenotypic continuum as it happens in many other lysosomal storage disorders[25] (Figure 3).

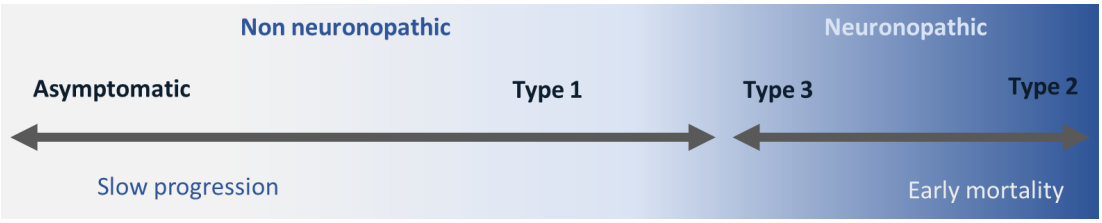


Figure 3: **GD symptoms represent a continuum.**

### 1.1.4 Diagnosis and therapeutic approaches

GD symptoms are relatively non-specific and heterogeneous, the disease onset is in general progressive and the diagnosis is often made many years after the onset of the first clinical and laboratory signs, causing in some cases poor response to therapies. Different algorithms have been drafted for early diagnosis of GD in pediatric patients, that can help clinicians in promoting a timely diagnosis and early access to therapy[26,27].

The suspicion of a GD diagnosis arises when a patient presents at least 2 symptoms between hepatosplenomegaly, thrombocytopenia, anemia, bone lesions and neurological involvement. The gold standard for diagnosis is the GCase enzyme activity assay starting from patients leukocytes or fibroblasts but also the more rapid and easy to manipulate whole

dried blood spot (DBS) is used to determine the enzymatic activity. In the GD patients the residual GCase activity is around the 10-15% of the normal values[28]. Apart from enzyme activity, other molecules, as chitotriosidase[29], glucosylsphingosin[30] and the lysosphingolipid hexosylsphingosine[31], have been proposed as potential biomarkers to diagnose and monitor the disease progression from both plasma and DBS. Bone marrow aspiration can also be performed on patients without a diagnosis when isolated thrombocytopenia and/or splenomegaly are found, even if it may be difficult to distinguish Gaucher cells from the "pseudo-Gaucher" cells observed in some blood disorders or infectious diseases, such as myeloma with histiocytic accumulation of immunoglobulin crystals[4]. The diagnosis is followed by the *GBA1* gene sequencing to look for the pathogenic mutations, useful also to provide a possible prognostic indication.

Standard of care currently consists of enzyme replacement therapy (ERT) with recombinant ß-glucocerebrosidase, which has been demonstrated to be safe and effective in preventing or reversing many clinical manifestations of GD type I, including hepatosplenomegaly, cytopenia, growth and bone disease[32,33]. However, the intravenous delivery of the enzyme is invasive, and the lack of uptake of GCase across the blood-brain barrier limits the potential of this approach in neuropathic diseases[34]. More recently, the substrate reduction therapy (SRT) was developed, aiming to restore the metabolic homeostasis between substrate and enzyme. The drugs target an earlier step in the GluCer metabolic pathway, leading to its production inhibition[35]. This approach has advantages when compared with ERT, including oral availability, non-immunogenicity, and the possibility to cross the blood-brain barrier, even if no effect have been seen on neuronopathic GD[36]. Another therapeutic approach is represented by pharmacological chaperone therapy (PCT), based on proteins able to bind the misfolded GCase and to induce conformational changes in the enzyme that can be correctly recognized by the endoplasmic reticulum and transported to the Golgi appartus and lysosomes[37]. Different classes of imminosugars, ambroxol and other non inhibitory molecules are currently under preclinical development and are promising especially for the treatment of neurological symptoms[38].

Luckily there are safe and effective strategies to prevent and reverse many clinical manifestations of GD, including hepatosplenomegaly, cytopenia, growth delay, and bone defects[39,33]. However, if diagnosis is delayed, some complications become irreversible, such as avascular bone necrosis, hepatic, splenic or bone marrow fibrosis and pulmonary hypertension, that occur in approximately 25% of GD patients. There is indeed a urgent need of new thera-

peutic approaches for non responsive patients and to treat the neuronopathic form of GD, currently without any therapeutic option.

## 1.2 Models to study GD

### 1.2.1 Animal models

Finding the right model to study the molecular mechanism behind the GD pathology onset has been a big challenge. The generation of animal models faithfully mimicking GD symptoms was not easy and the ideal model is still not available.

The first attempt to establish a GD mouse model involved the intraperitoneal injection of the irreversible GCase inhibitor, conduritol B epoxide (CBE) to mice. After 3 weeks GCase activity was strongly inhibited and accumulation of GlcCer in the spleen, liver and brain was reported [40]. Further augmentation of GlcCer levels was later achieved by injecting mice with a mixture of CBE and GlcCer. Although this chemically induced model has not been widely used, it is a relatively quick and inexpensive model that could potentially be used more extensively to examine neurological defects and to test the efficacy of novel therapies [41]. The first genetic mouse model of GD was produced in 1992 by the insertion of a neomycin cassette in exons 9 and 10 of the *GBA1* gene, which generated a mouse carrying a *GBA1* null mutation resulting in a very strong GD phenotype, with a residual enzyme activity lower than 4%, comparable to type 2 GD patients [42]. The short lifespan of this knock-out (KO) mouse is the main negative aspect of the model, even if some studies on the neuronopathic GD forms were performed [43]. The attention was then focused on the development of less severe mouse models of GD carrying *GBA1* point mutations. Through a single insertion mutagenesis procedure a mouse model carrying the homozygous L444P mutation and one carrying the recombinant allele RecNCil were generated [44]. Both strains died soon after birth probably because of the severe compromised skin barrier function rather than because of the neurological defects. No evident phenotypic abnormalities were instead observed in mice with the D409H, D409V or V394L *GBA1* point mutations, even though the residual GCase activity was only 4–10% of the wild type one. Only low levels of GlcCer accumulation were detected in the spleen of these mice and hepatosplenomegaly was not observed. Surprisingly mice carrying N370S mutation, associated with mild phenotypes in humans, die within 24 hours of birth owing to a skin defect, similar to *GBA1* KO mice [45]. The generation of a conditional GD mouse model represented the major breakthrough in the development of GD mouse

models. Both GD type I and neuronophatic GD characteristic are well recapitulated by different Cre-LoxP mouse models[46,47,6].

Since the generation of a GD mouse model was not so easy and effective, other less complex animal models have been taken into account to investigate GD pathogenesis.

The fruit fly Drosophila melanogaster has been considered a good candidate since mutations or the complete KO of the *GBA1* ortholog gene (*GBA1b*) are causative of the same alterations seen in humans[48,49,50,51]. A Drosophila model lacking the two fly *GBA1* orthologs was shown to recapitulate the main GD features at cellular level with severe lysosomal defects and accumulation of glucosylceramide in the fly brain[49]. More recently, *GBA1b* mutant flies giving rise to a mutant GCase protein, missing 33 C-terminal amino acids were generated. These flies presented a significant decrease in GCase activity with concomitant substrate accumulation, activation of the unfolded protein response, inflammation and neuroinflammation that lead to the development of a neuronopathic disease form[51].

Also in the Zebrafish genome the ortholog of human *GBA1* gene (*Gba1*) is present and its deletions or alterations cause marked sphingolipid accumulation, Gaucher cells invasion and microglial activation. Both inhibitory and genetic models have been developed. Not only CBE but also cyclophellitol derivatives are indeed potent and selective *Gba1* inhibitors in Zebrafish that could generate reliable GD models[52]. *Gba1* loss of function can be generated through different strategies including splicing-blocking morpholino oligo[53] and TALEN or CRISPR/Cas9 based genome editing[54,55].

### 1.2.2 iPSC and disease modelling

A big breakthrough in the GD modelling came up with the discovery of induced pluripotent stem cell (iPSC) in 2006. Yamanaka and colleagues reported for the first time the possibility to reprogramme terminally differentiated and lineage restricted adult somatic cells to a pluripotent state through the forced ectopic expression of the transcriptional factors Oct4, Sox2, Klf4, c-myc, Nanog and Lin28[56]. They can be easily generate starting from fibroblast or mononuclear peripheral blood of patients or healthy donors and they exhibit similar gene expression, epigenetic profile and differentiation potential that of embryonic stem cells[57] (Figure 4). iPSC technology has attracted a considerable interest for its potential applicability in personalized regenerative medicine and in disease modelling, particularly as a drug discovery tool for genetic diseases and in neurodegenerative pathologies. Even if iPSC can not

reproduce the systemic complexity as an animal model, they are a really powerful tool enabling the study of specific cell subtypes primarily involved in the pathology retaining genetic risk variants directly derived from patients. iPSC can be easily manipulated through genome editing techniques, propagated in culture and differentiated towards the desired fate. More recently many different protocols have been developed to generate iPSC-derived 3D culture systems mimicking in an always more precise way the human tissues and organs physiology. Different kinds of brain, intestinal, liver, kidney organoids can be easily obtained from iPSC differentiation[58,59,60,61]. These iPSC-derived organoid structures seem to well recapitulate the brain 3D cytoarchitectural arrangement and provide new opportunities to explore disease pathogenesis and can serve as a preclinical platform to bridge the translational gap between animal models and human clinical trials[58].

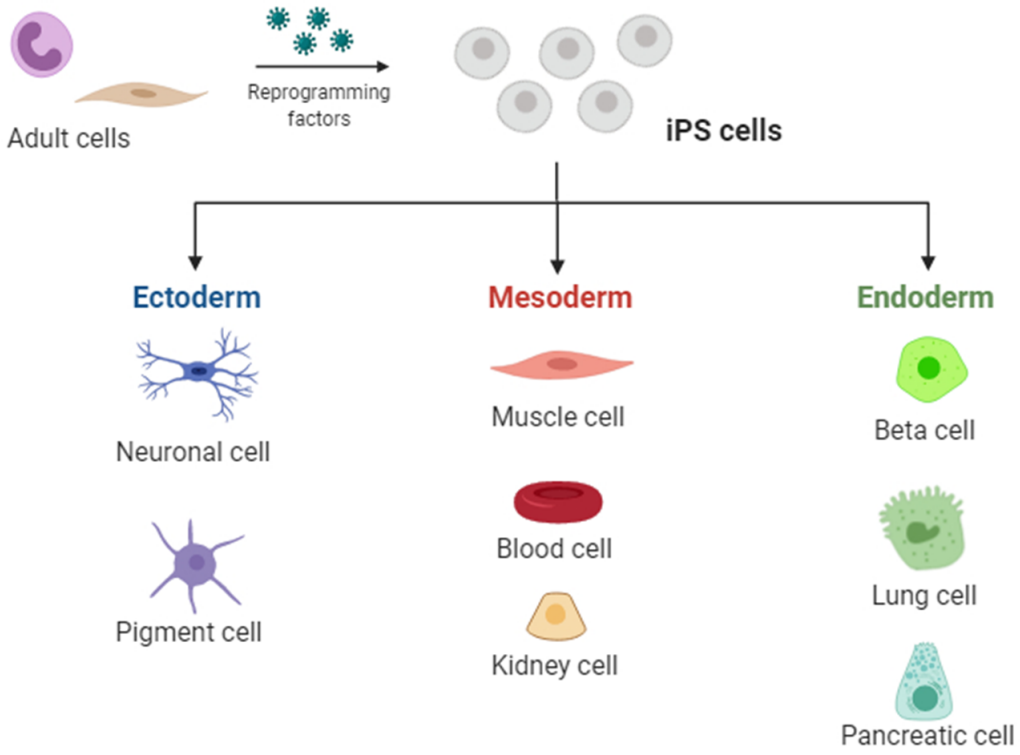


Figure 4: **iPSC generation and differentiation potential.**

### 1.2.3 iPSC in lysosomal storage disorders

The development of patient-derived iPSC had a big impact on lysosomal storage disorder research. iPSC lines derived from patients affected with the most common lysosomal storage disorders (Gaucher disease, Fabry disease, Pompe disease, Niemann-Pick types A and

C1, metachromatic leukodystrophy and several of the mucopolysaccharidoses) have been already generated[62]. They were proved to be able to faithfully recapitulate disease characteristics, biochemical and cellular features, giving novel opportunities to clarify the disease ethiopathology and to test new therapeutic strategies. The cell types primary affected by lysosomal storage disorders belong to the neuronal and hematopoietic lineages, which are indeed the iPSC differentiation targets reported in the majority of the studies published in the field[62]. Each differentiated cell type closely resembles the primary disease phenotypes and represents the best model to investigate the consequences of the sphingolipids storage in the cell lysosomes and cytoplasm. Moreover, the genetic manipulation of these cells, through gene correction of the causative mutation or the introduction of new pathogenic alterations, is functional in understanding the specific roles of causative genes and the contributions of other genetic factors to the disease phenotypes[63].

In particular, iPSC have recently proved to be a valuable tool to study specific cell populations in GD, showing sphingolipid accumulation and low levels of GCase[64]. Different iPSC lines have been derived from type 1, 2 and 3 GD patients and they have been efficiently differentiated towards the macrophage[65], neuronal[66,67,68] and osteoblast[69] fate. Many other studies exploiting iPSC have been performed using lines reprogrammed from PD patients carrying heterozygous *GBA1* mutations[70,71,72].

The use of iPSC model allowed new insights into many aspects of GD molecular and cellular pathology. Alterations in different cell mechanisms, including inflammatory response, autophagic flux, lysosomal activity, calcium signaling and $\alpha$-synuclein accumulation have been linked to GCase deficit and GluCer accumulation[73].

# 2 Aim of the study

Even if GD is considered a monogenic disease, it is characterized by a wide spectrum of clinical manifestations, also among individuals with the same mutational event within the *GBA1* gene; some patients present a systemic symptomatology with moderate visceral involvement while others are affected by a more severe neurological form. It is therefore increasingly important to identify genes that could have a role in the modulation of the phenotype and in the worsening of the disease course. The project carried out as part of the three-year PhD program aimed to develop a relevant and reliable disease model to investigate alterations of genes or entire pathways that act in synergy with *GBA*1 mutations when the disease occurs. The study of the mechanisms underlying the onset of the different GD forms has been carried out through iPSC derived from patients and healthy donors. To have a proper comparison model, healthy control cells have been treated with the irreversible GCase inhibitor CBE and patient-derived iPSC have been genetically modified with the correction of the causative mutations by genome editing. The comparison of the GD lines with the isogenic gene corrected counterparts represents indeed the best approach to explore common pathways evoked or disrupted by the pathogenic mutations. iPSC have been differentiated towards the monocyte/macrophage fate, to study in the hematologic compartment the mechanisms trigging the inflammation response, and to dopaminergic neurons to evaluate the signaling pathways linked to neurodegeneration and neuroinflammation activated by GCase enzyme dysfunction and substrates accumulation. The identification of molecular targets involved in unrestrained inflammation and neuronal cell death that drive the most severe manifestations of the disease could be instrumental in the development of new pharmacological approaches to GD that are urgently required especially for neuronopathic patients that do not benefit from standard therapy.

# 3 Materials and methods

## 3.1 iPSC lines generation

iPSC have been generated from the peripheral blood mononuclear cells (PBMCs) of two GD type 1 patients, one compound heterozygous for the N370S and L444P mutations and one homozygous for the N370S. After blood collection, mononuclear cells have been isolated through Ficoll (Lymphoprep) gradient centrifugation, collected and counted diluted in the nigrosin dye in a Burker chamber. Sendai vectors encoding for the reprogramming factors: Klf4, cMyc, Sox2 and Oct4 from the CytoTune™-iPS 2.0 Sendai Reprogramming Kit (ThermoFisher) have been used. According to the manufacturer instructions, PBMCs have been seeded in a 24 well plate and kept in culture for 3 days in PBMC medium (Table 1). $5 \times 10^5$ cells have been then collected in a round bottom tube and resuspended in PBMC medium containing the viruses. After a 30 minutes centrifugation step at 1000g to optimize the infection rate, cells have been seeded in a 12 well plate already containing 1 mL of fresh PMBC medium. The infection has been performed with a MOI of 5 for Oct4, Sox2 and c-myc and of 3 for Klf4. The following day the medium with the cells has been collected and centrifuged in order to remove the viral particles, the cells have been seeded again in a 24 well plate. After 2 days in culture, cells have been counted again and seeded with 1 x $10^4$ - 1 x $10^5$ live cells per well in 2 mL of complete StemPro-34 (ThermoFisher) medium onto vitronectin (ThermoFisher) coated B35 plates (Falcon). After 3 days in culture in complete StemPro-34, cells have been transitioned to Essential 8 (ThermoFisher), the iPSC growth medium. Medium has been changed daily and after aproximately one week in culture the first iPSC colonies started to emerge. The pluripotency of the cells colonies has been tested in live staining through TRA 1-60 antibody (ThermoFisher), only the positive colonies have been harvested and transferred in a new vitronectin coated plate for amplification and further characterization.

### 3.1.1 iPSC model validation

To check that any chromosome alteration has occurred during the reprogramming, cells karyotype was evaluated before and after the process. Karyotype was analysed through the G-banding technique, in which cells fixed in glacial acetic acid and methanol (1:3), are treated with trypsin, a proteolytic enzyme able to digest histone proteins and then put in a Giemsa

| Medium | Composition | Supplements | Concentration |
|---|---|---|---|
| PBMC medium | StemPro-34 | SCF | 100 ng/mL |
| | | FLT3 | 100 ng/mL |
| | | IL3 | 20 ng/mL |
| | | IL6 | 20 ng/mL |
| | | L-glutamin | 2nmM |
| | | Company supplement | |
| Complete StemPro-34 | StemPro-34 | L-glutamine | 2 mM |
| | | Company supplement | |
| Essential 8 medium | Essential 8 | Company supplement | |

Table 1: **iPSC reprogramming media.** List of medium composition and supplements used for the reprogramming of PBMCs to iPSC.

solution which colours the digested regions rich of condensed chromatin, giving as a result a specific banding pattern. The pluripotency of the cells has been tested through embryoid bodies (EB) formation; iPSC have been seeded in single cell in ultra low attachment plates (StemCell) in Essential 6 medium (ThermoFisher). After 7 days in culture they spontaneously generated small bodies structures which have been kept in culture for another week. The presence of the three germinal layers structure has been evaluated through quantitative Real Time PCR (qRT-PCR) performed on the RNA extracted from the EB structure after 14 days in culture. Primers for endoderm, mesoderm and neuroectoderm specific expressed genes have been used (Table 2).

## 3.2 iPSC culture

iPSCs colonies were cultivated in Essential 8 medium in vitronectin coated B35 plates (Falcon). For standard passaging, cells were washed once with DPBS, incubated for 2 minutes in a solution of DPBS with 0.5mM EDTA, detached in 1 mL of fresh medium and transferred in a new coated plate. For procedures requiring the single cell condition, after PBS washing, cells have been incubated with 1 mL of accutase (ThermoFisher) for 5 minutes at 37°C . Once detached, accutase was diluted with 5mL of DMEM-F12 medium (Gibco) and the cells were collected and centrifuged for 5 minutes at 300g in a 15 mL tube. Cells were then resuspended in the final medium supplemented with ROCK inhibitors Y27632 10$\mu$M (Miltenyi). iPSC have been frozen in KnockOut Serum (ThermoFisher) with 10% DMSO.

| Gene | Marker for | Primers |
|---|---|---|
| NANOG | Pluripotency | F: 5’ - CCATCCTTGCAAATGTCTTCTG - 3’<br>R: 5’ - CTTTGGGACTGGTGGAAGAATC - 3’ |
| OCT4 | Pluripotency | F: 5’ - GCAGCAGATCAGCCACATC - 3’<br>R: 5’ - CTTGATCGCTTGCCCTTCT - 3’ |
| AFP1 | Endoderm | F: 5’ - CAAAATGCGTTTCTCGTTGCT - 3’<br>R: 5’ - GCTGCCATTTTTCTGGTGATG - 3’ |
| FOXA2 | Endoderm | F: 5’ - CCACCTGAAGCCGGAACA - 3’<br>R: 5’ - TGCTCCGAGGACATGAGGTT - 3’ |
| GATA4 | Endoderm | F: 5’ - GCTATGCGTCTCCCGTCAG - 3’<br>R: 5’ - GTGACTGTCGGCCAAGACC - 3’ |
| HAND1 | Mesoderm | F: 5’ - AACTCAAGAAGGCGGATGG - 3’<br>R: 5’ - AGGGCAGGAGGAAAACCTT - 3’ |
| MIXL1 | Mesoderm | F: 5’ - GGTACCCCGACATCCACTTG - 3’<br>R: 5’ - TAGCCAAAGGTTGGAAGGATTTC - 3’ |
| NEUROD1 | Neuroectoderm | F: 5’ - GAGCACGAGGCAGACAAGAAG - 3’<br>R: 5’ - CCCCCGTTCCTCAGTGAGT - 3’ |
| PAX6 | Neuroectoderm | F: 5’ - CCGCCCTGGTTGGTATCC - 3’<br>R: 5’ - TTGGTATTCTCTCCCCCTCCTT - 3’ |
| SOX1 | Neuroectoderm | F: 5’ - ATGAAGGAGCACCCGGATTA - 3’<br>R: 5’ - CTTCTTGAGCAGCGTCTTGGT - 3’ |

Table 2: **Embryoid bodies primer list.** Primers used to check the expression levels of the pluripotency and germinal layers markers in the iPSC-derived EB.

## 3.3 CBE treatment

An already reprogrammed and characterized healthy donor-derived iPSC line was used as control in many experiments. Once differentiated, these cells have been treated with the GCase inhibitor, CBE for 3 to 9 days with a variable concentration (250$\mu$M for hematopoietic differentiated cells and 100$\mu$M for neural precursor cells (NPC) and neurons) depending on the experiment aim and conditions.

## 3.4 Gene correction

GD-iPSCs have been gene corrected in order to obtain an isogenic control model. The genome editing strategy took advantage of a zinc finger nuclease (ZFN) mediated homologous recombination system, aiming to introduce a neomycin selection cassette in *GBA1* intron 9-10 and to correct both N370S and L444P mutations in exon 9 and 10 respectively developed in the laboratory of Prof Deleidi[70]. The wild type sequence is present in the left and right homology arm of the construct, flanking the selection cassette under control of the constitutive PGK promoter. iPSC have been dissociated in single cell, collected in Essential 8 medium and 1.5 x $10^6$ have been centrifuged and transfected with 0.83$\mu$g of each ZFN construct (Sigma), as well as 3.3$\mu$g of the linearized *GBA1* targeting vector. The stem cell Nucleofector Kit (Lonza) with the program B016 of Amaxa Nucleofector I (Lonza) were used for transfection. Cells were then plated in 10 cm coated plates in Essential 8 medium with 10$\mu$M ROCK inhibitors. Medium has been changed every day and, after the formation of small colonies, the antibiotic G418 250$\mu$g/ml (Biochrom) was added to select the clones carrying the homologous recombination. Resistant colonies have been transferred in a new coated 12 well plate for expansion and further characterization through target sequencing.

### 3.4.1 DNA extraction and amplification

DNA was extracted from isolated clones using the QIAamp DNA Mini kit (Qiagen). The quantification was performed with the NanoDrop 1000 spectrophotometer (Thermo Scientific), evaluating the absorbance at 260 nm. Samples purity was established by the absorbance 260/280 and 260/230 ratio.

The primers on the *GBA1* sequence have been drawn with the Primer Express software in the regions with the highest number of mismatch among gene and pseudogene, while the

primers on the neomycin cassette are already published[70]. The sequence of the whole *GBA1* gene was obtained from the genome browser Ensembl and the primers specificity was verified using Primer Blast software (Table 3).

| Region | Mutation | Primers | Annealing T |
|---|---|---|---|
| *GBA1* intr 9-10<br>Neomycin cassette | N370S | F: 5' - CACACCCCCAACTCCTTAGCTA - 3'<br>R: 5' - CTCGACGAAGTTCCTATTCCG - 3' | 62°C |
| Neomycin cassette<br>*GBA1* intr 11-12 | L444P | F: 5' - CTGGGGGAAGTTCCTATTCC - 3'<br>R: 5' - CAGGATCACACTCTCAGCTTCTCC - 3' | 62°C |

Table 3: **List of primers used for colonies screening.** The primer target a region between the *GBA1* gene and the neomycin cassette both upstream and downstream in order to check that the proper recombination event has occurred.

PCR was performed using the FastStart Taq DNA Polymerase kit (Roche) according to the manufacturer instruction, for each sample 1 $\mu$l of 10ng/$\mu$L DNA was incubated with 24 $\mu$l of reaction mix. The reaction took place in a thermocycler with the following program: 95°C for 5 min, (95°C for 30 sec, 62°C for 30 sec, 72°C for 1 min) for 40 cycles, 72°C for 7 min. To check for the presence of the amplified segment, 3 $\mu$l of each PCR product with 2 $\mu$l of bromophenol blue were loaded in a 1.5% agarose electrophoresis gel with the nucleic acid stain GelRed (Biotium) 1:1000.

### 3.4.2 Clones sequencing

If the right molecular weight bands were present both upstream and downstream the cassette integration site, the samples have been sequenced by Sanger procedure to check for the effective gene correction of the mutation and the absence of mismatches in the region both at DNA and cDNA levels. The PCR products were purified using the MultiScreen-PCR96 filter plate (Millipore) connected to a vacuum pump set to 100 mbar. 70 $\mu$l of $H_2O$ were added to each sample and the whole solution was transferred into the plate. After 10 minutes of aspiration, 30 $\mu$l of $H_2O$ were added to the PCR products attached to the membrane of each well and resuspended though mechanical vortexing. The BigDye Terminator v1.1 Cycle Sequencing kit (Applied Biosystems) was used to prepare the sequencing mix. The reaction took place into a thermocycler with the following program: 96°C for 30 sec, (96°C for 10 sec, 60°C for 4 minutes) for 25 cycles. The sequenced DNA has been purified with a sodium acetate based precipitation protocol. Before the lecture with the 96-capillary ABI

3730 DNA Analyzer (Applied Biosystems), each purified precipitate was resuspended into 10 $\mu$l of Injection Buffer (Millipore). The sequences were read as electropherograms with the Sequencher 4.1 software (Gene Codes Corporation).

## 3.5 Monocyte-macrophage differentiation

iPSC were differentiated towards the monocyte/macrophage fate using a 2D co-culture system on matrix adapted from Chou et al.[74]. Briefly 5-6 colonies of each iPSC line were picked and put into Geltrex (Thermofisher) coated wells in Essential 8 medium. The day after the medium was replaced with StemPro34 medium (Thermofisher) enriched with 1X penicillin/streptomycin (Gibco), 2mM glutamine (Gibco), 50 $\mu$g/ml ascorbic acid (Sigma), 15 mM monothioglycerol (Sigma) and the cytokines required in the day 0 of the differentiation (Table 4). The medium was replaced every two days until day 18 with a cytokine cocktail specific for every time point of the differentiation, as shown in Table 4. At day 7, hematopoietic precursors start to emerge from the underlying mesenchymal cells. Hematopoietic differentiation of iPSC was then assessed at day 13, 15 and 18 of the differentiation through flow cytometry analyses, checking the positivity for the hematopoietic precursors markers (CD34, CD43, CD45) and monocyte/macrophage lineage markers (CD11b, CD14 and CD163). All samples were analyzed through the FACSCantoII flow cytometer and the data analyzed with the FlowJo software (BD). Antibodies were purchased from BD and all the cytokines from Peprotech.

## 3.6 Neuronal differentiation

To generate mature midbrain dopaminergic (mDA) neurons, iPSC were first differentiated towards the neural precursor cell (NPC) fate. Colonies have been cut and detached 3-4 days after splitting, resuspended in hESC - medium (Table 5) supplemented with the following small molecules: 10$\mu$M SB-431542 (TGF$\beta$ signaling inhibitor) 1$\mu$M dorsomorphin (DM - BMP pathway inhibitor), 3$\mu$M CHIR-99021 (canonical Wnt signaling pathway activator), 0.5$\mu$M puromorphamine (PMA - SHH pathway stimulator) and transferred to a new 6 well plate. After 2 days in culture, colonies start to form embriod bodies (EB) structure in suspension and the medium is carefully change to N2-B27 with the 4 small molecules supplement. After 2 other days in culture, the medium is changed to NPC maintenance medium (Table 5). At the 6th day of the differentiation protocol, the EB were collected, triturated and seeded in

| Day | BMP4 | CHIR | VEGF | bFGF | SCF | Flt3L | IL3 | M-CSF | GM-CSF |
|---|---|---|---|---|---|---|---|---|---|
| 0 | 5ng/mL | 930ng/mL | 50ng/mL | | | | | | |
| 1 | 5ng/mL | | 50ng/mL | 20 ng/mL | | | | | |
| 4 | | | 15ng/mL | 5 ng/mL | | | | | |
| 6 | | | 50ng/mL | 50 ng/mL | 50ng/mL | 5ng/mL | | | |
| 7 | | | 50ng/mL | 50 ng/mL | 50ng/mL | 5ng/mL | 25ng/mL | 50ng/mL | |
| 8 | | | 50ng/mL | 50 ng/mL | 50ng/mL | 5ng/mL | 25ng/mL | 50ng/mL | 25ng/mL |
| 11 | | | 50ng/mL | 50 ng/mL | 50ng/mL | 5ng/mL | 25ng/mL | 50ng/mL | 25ng/mL |
| 13 | | | 50ng/mL | 50 ng/mL | 50ng/mL | 5ng/mL | 25ng/mL | 50ng/mL | 25ng/mL |
| 15 | | | 50ng/mL | 50 ng/mL | 50ng/mL | 5ng/mL | 25ng/mL | 50ng/mL | 25ng/mL |
| 18 | | | 50ng/mL | 50 ng/mL | 50ng/mL | 5ng/mL | 25ng/mL | 50ng/mL | 25ng/mL |

Table 4: **List of cytokines for the monocyte/macrophage differentiation.** The different cytokines have been added to the enriched StemPro34 medium for the differentiation of the iPSC towards the mature fate.

a Matrigel (Corning) coated 12 well plate in NPC maintenance medium with ROCK inhibitors Y27632 10$\mu$M (Miltenyi). At this stage cells express neural progenitor markers and, once disaggregated, form homogeneous colonies of neuroepithelial cells. These NPC can be split enzymatically without manual selection at a 1:10 to 1:20 ratio and expanded as cell lines for more than 100 doublings[75].

To obtain mature mDA neurons, 1 million NPC have been seeded in a 6 well plate in NPC maintenance medium. After 2 days in culture the ventral nervous system differentiation stimulus is induced by increasing the PMA concentration and adding FGF8 to the N2-B27 medium. After 8 days in this differentiation medium, a cytokines cocktail containing: BDNF, GDNF, TGF$\beta$3, dbcAMP and Ascorbic Acid was used for the maturation of neurons. After 2 weeks in maturation conditions, with medium change every 3 days, neurons are ready for the experiments[75].

## 3.7 Growth rate evaluation

Cell growth potential was evaluated both for mature monocyte/macrophage cells and NPC. CD43 + hematopoietic differentiated cells (at day 15 of the differentiation protocol) were seeded both in methylcellulose (H4230, StemCell Technologies - 50000 cells per condition in a 6 well plate) and in the basal differentiation medium (100000 and 200000/well in a 12 well plate) enriched with the proper cytokine cocktail and the growth rate was evaluated

| Medium | Composition | Supplements and cytokines | Concentration |
|---|---|---|---|
| hESC - | DMEM KO (75%) | L-glutamin | 2mM |
| | KnockOut serum (25%) | Pen/Strep | 1:100 |
| | | Non essencial aminoacids | 1:100 |
| | | $\beta$ -Mercapto | 25mM |
| N2-B27 | DMEM F12 (50%) | L-glutamin | 2 mM |
| | Neurobasal (50%) | Pen/Strep | 1:100 |
| | | N2 | 1:100 |
| | | B27 | 1:100 |
| NPC maintenance | N2-B27 | CHIR-99021 | 3$\mu$M |
| | | PMA | 0.5$\mu$M |
| | | Ascorbic Acid | 150$\mu$M |
| Differentiation | N2-B27 | FGF8 | 100ng/mL |
| | | PMA | 1$\mu$M |
| | | Ascorbic Acid | 200$\mu$M |
| Maturation | N2-B27 | BDNF | 10ng/mL |
| | | GDNF | 10ng/mL |
| | | TGF$\beta$3 | 1ng/mL |
| | | dbcAMP | 500$\mu$M |
| | | Ascorbic Acid | 200$\mu$M |

Table 5: **Media for neuronal differentiation.** List of medium composition and cytokines required for the differentiation of iPSC towards the midbrain dopaminergic fate.

after 6 days for three weeks for the semisolid growth condition and every three days in liquid culture. To evaluate the growth rate of NPC, they have been seeded at two different densities (100000 and 200000/well in a 12 well plate) in the standard maintenance culture medium and the cell number was evaluate after 3, 6 and 9 days in culture.

## 3.8 Cell death evaluation

Cell death and apoptosis have been analysed through flow cytometry (MACSQuant Analyzer, Mylteni); NPC have been detached with accutase, washed once with PBS and stained with propidium iodide (PI) and AnnexinV (FITC) for 30 minutes in PBS 4% FBS before the acquisition.

## 3.9 Gene expression analysis

Total RNA was extracted by RNeasy spin column method (Qiagen). 250 ug of RNA were reverse transcribed to cDNA through the Transcriptor first strand cDNA synthesis kit (Roche Diagnostics) with oligo-dT primers (2.5 M). qRT-PCR was performed with FastStart Sybr Green Master Mix (Roche Diagnostics) on the LightCycler 480 apparatus (Roche Diagnostics) using specific primers for the target genes (Table 6). DDCt method was used to quantify gene expression levels normalized on three housekeeping genes: GAPDH, ATPS and RLP0.

## 3.10 Immunofluorescence stainings

Cells have been fixed in 4% paraformaldehyde for 15 minutes, rinsed twice with PBS and blocked with 10% normal goat serum in PBS+0.1% TritonX-100 for 1 hour. Primary antibody incubation was performed overnight at 4° while secondary antibody incubation lasted 2 hour at room temperature with the appropriate species of Alexa Fluor488/568-conjugated antibody (Invitrogen). Cell nuclei were counterstained with DAPI (Biozol - 1:10000). Anti $\beta$3-Tubulin primary antibody (mouse, BioLegend, #MMS-435P) was used 1:1000, anti Tyrosine Hydroxylase (TH, rabbit, Pel-Freeze, #P40101-150) 1:500 and YAP (rabbit, Cell Signaling Technology, #14074) 1:100. Pictures have been acquired with the Leica TCS SP8 confocal microscope (Leica), analyzed with Fiji software and brightness/contrast was adjusted equally. Nuclear localization of YAP in NPC and neurons was evaluated with the Intensity Ratio Nuclei Cytoplasm Tool plug-in of the Fiji software.

| Gene | Pathway | Primers |
|---|---|---|
| RIP1 | Necroptosis | F: 5’ - GCAGTACCTTCAAGCCGGTC - 3’<br>R: 5’ - GCAAACCAGGACTCCTCCAC - 3’ |
| RIP3 | Necroptosis | F: 5’ - ACCCCGGAGCCAAATCC - 3’<br>R: 5’ - AGCCCCTCCCCTTGCC - 3’ |
| MLKL | Necroptosis | F: 5’ - TCACACTTGGCAAGCGCATGGT - 3’<br>R: 5’ - GTAGCCTTGAGTTACCAGGAAGT - 3’ |
| ANKHD1 | Hippo | F: 5’ - CCTGCTTGGAACCCTATGATAAA - 3’<br>R: 5’ - CGTGCCAGGCCAAATCTG - 3’ |
| CTGF | Hippo | F: 5’ - CCGCCTGTGCATGGTCA - 3’<br>R: 5’ - GGTGCAGCCAGAAAGCTCA - 3’ |
| CYR61 | Hippo | F: 5’ - TTTGTGAGGTGCGGCCTT - 3’<br>R: 5’ - CTTGGGCCGGTATTTCTTCA - 3’ |
| ATPS | Housekeeping | F: 5’ - GTCTTCACAGTTCATATGGGGA - 3’<br>R: 5’ - ATGGGTCCCACCATATAGAAGG - 3’ |
| GAPDH | Housekeeping | F: 5’ - AGGGGAGATTCAGTCTGG - 3’<br>R: 5’ - CGACCACTTTGTCAAGCT - 3’ |
| RLP0 | Housekeeping | F: 5’ - CCTCATATCCGGGGGAATGTG - 3’<br>R: 5’ - GCAGCACTGGCACCTTATTG - 3’ |

Table 6: **List of qRT-PCR primers.** Sequence of the primers used to evaluate the expression levels of necroptosis and Hippo pathways effectors and the relative housekeeping genes.

# 4 Results

## 4.1 Establishment of GD patients-derived iPSC lines

Two patients affected by type 1 GD have been enrolled in the study, the first one presented a compound heterozygous condition in the *GBA1* gene for the N370S and the L444P mutations (GD-1), while the second one had the N370S on both alleles (GD-2). PBMCs of the two GD patients have been isolated and reprogrammed to the pluripotent state through the Sendai vectors infection. Two weeks after the infection the first iPSC-like colonies started to emerge from the culture. To prove their pluripotent state, cells have been stained with the TRA 1-60 conjugated primary antibody, optimized for live staining. Both patients lines showed positive colonies (Figure 5A) that have been picked and expanded in iPSC medium. iPSC model validation and characterization has been performed checking both the wild type kayotype maintenance before and after the reprogramming process and their ability to spontaneously differentiate into EB structure in low attachment culture condition. To prove the potency of these cells, EB have been disgregated after 14 days in culture and the expression levels of pluripotency and germinal layers markers have been evaluated. qRT-PCR data show a strong decrease in the pluripotency markers levels if compared with the iPSC state, while all the mesoderm, endoderm and neuroectoderm markers are strongly increased (Figure 5B).
An already characterized healthy donor-derived iPSC line (CNTR) has also been exploited in the study. To generate a GD-like condition, these cells have been treated with the GCase irreversible inhibitor CBE, inducing GCase substrates accumulation.

## 4.2 GD-iPSC efficiently differentiate towards the macrophage fate

The GD-1 iPSC together with the CNTR line were amplified and subsequently differentiated into hematopoietic precursors and then monocyte/macrophage cells through a 2D co-culture system on matrix (Figure 6A). From day 10 of the differentiation protocol CNTR cells were treated with CBE 250$\mu$M to obtain a further comparison model. At day 12 of differentiation the supernatant containing the precursors cells was collected and lineage specific markers were tested through flow cytometry. Both the CNTR, CNTR treated with CBE and GD-1 lines are able to give rise to CD34, CD43 and CD45 positive hematopoietic progenitor cells and the efficiency of the differentiation procedure seemed to be higher in the GD model (Figure 6B). This effect was even more evident when the immunophenotype was evaluated

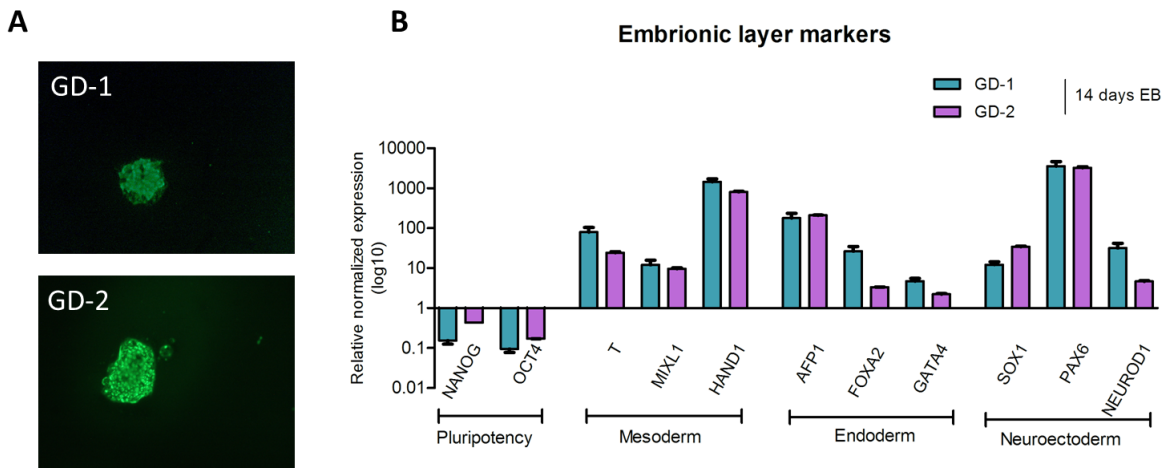


Figure 5: **GD iPSC lines characterization.** A) TRA 1-60 positive colonies (green) of GD-1 and GD-2 iPSC lines. B) Expression levels of the embryonic layer markers evaluated through qRT-PCR after spontaneous formation of EB structure in GD iPSC; while the pluripotency markers Nanog and Oct4 decrease in both the populations, all the analysed germ lineage markers increase in the embryoid body state. All data are normalized on iPSC expression level.

at day 19 of differentiation when the cells are positive for the mature lineage markers CD11b, CD14 and CD163. Interestingly, GD-1 line expressed significantly higher levels of all the analysed markers if compared with the CNTR line. Also cells treated with CBE showed the same trend suggesting that GD cells may have an higher differentiation efficiency (Figure 6C).

## 4.3 GD iPSC-derived monocyte/macrophages display a growth defect

At day 15 of the differentiation protocol CD43+ cells have been collected and seeded both in semisolid and liquid culture conditions enriched with specific hematopoietic cytokines to check for their self-renewal properties and proliferative rate. After 6 days in methylcellulose the number of emerged colonies has been counted and the cells have been replated in the same conditions. Already from the first time point, CNTR cells treated with CBE and GD-1 cells showed a lower capacity to give rise to colonies, a condition that became more evident after the first and the second replating (Figure 7A). A similar situation was evident also in the liquid culture analysis where iPSC-derived monocyte/macrophages have been counted and replated every three days. The growth defect of GD lines compared with CNTR is statistically significant and seemed to be closely related to the enzymatic defect since the treatment with CBE caused a deficit similar to the patient-derived cells (Figure 7B).

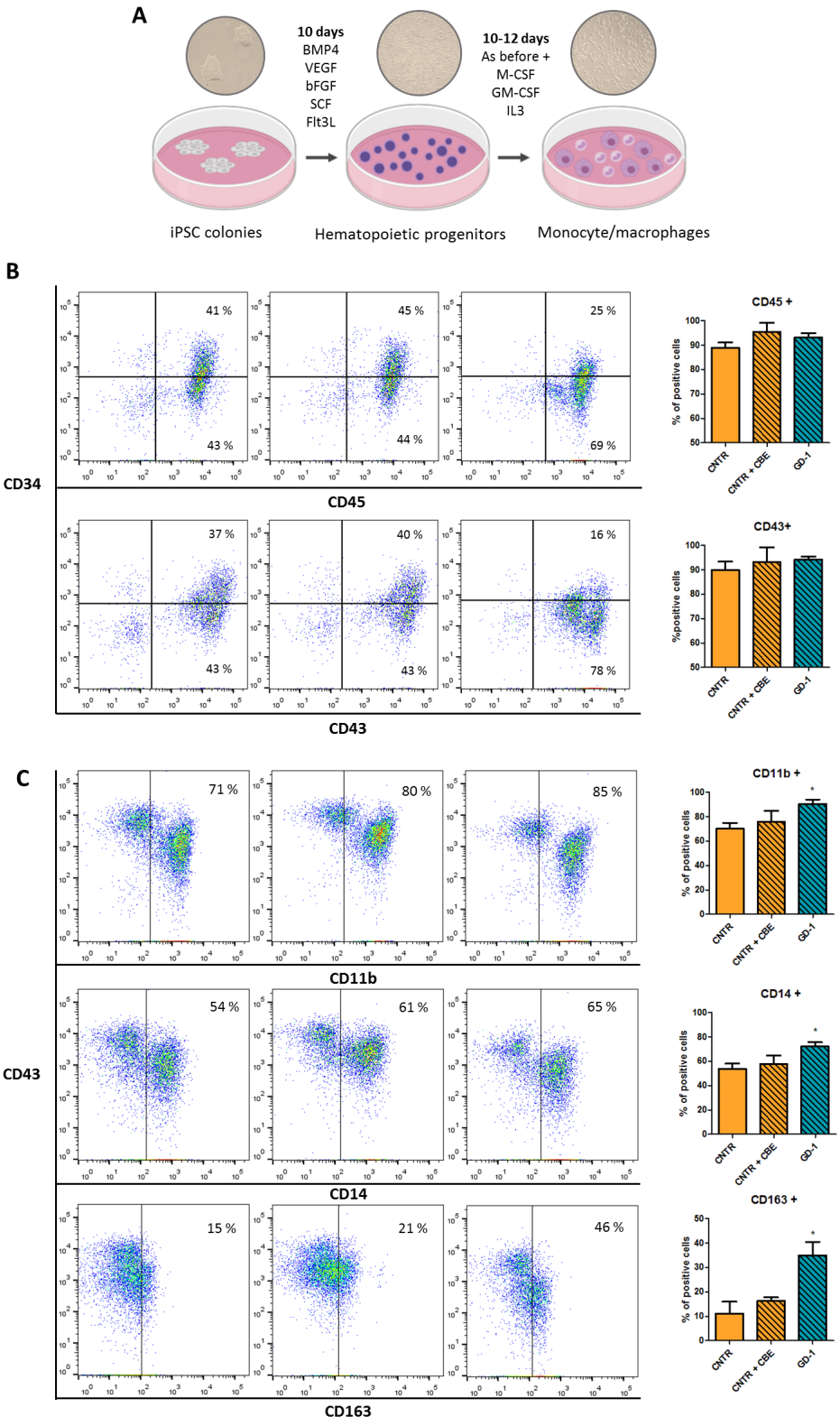


Figure 6: **Flow cytometry evaluation of iPS cells during the monocyte/macrophage differentiation.** A) Schematic representation of the differentiation protocol with the main cytokines. B) At day 12 of differentiation the majority of the cells express the hematopoietic progenitors markers CD34, CD43 and CD45. C) The positivity of the monocytic markers CD11b and CD14 and the mature macrophage marker CD163 at day 19 of differentiation is shown. Statistical significance is indicated as p-value (Student's t-test), $p<0.05$, n=3.

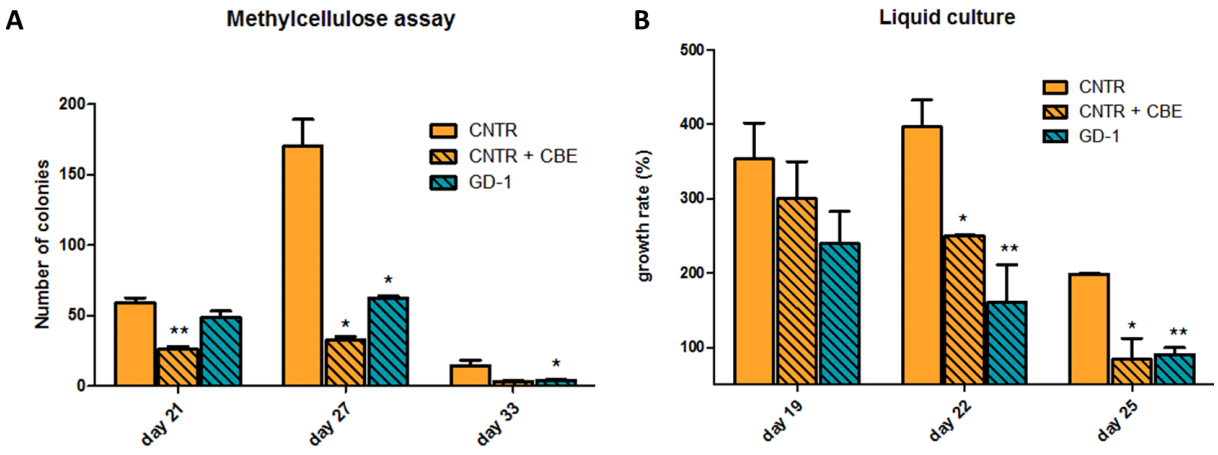


Figure 7: **Growth rate evaluation in iPSC-derived monocyte/macrophage cells.** A) Representation of the number of colonies generated in the methylcellulose culture conditions for the three lines after the first, second and third replatements. B) Cell count of differentiated cells in liquid culture. Statistical significance is indicated as p-value (Student's t-test), * $p<0.05$, ** $p<0.005$, n=3.

## 4.4 Necroptosis pathway is hyperactivated in GD monocytes/macrophages

A reduction in the growth rate can be explained both with a decrease in cell proliferation or an increase in cell death induction. As the triggering of inflammatory mechanisms and the release of cytokines are common features of GD pathophysiology[76,77,78], we hypothesized that a cell death mechanism activated by inflammation could be an interesting involved pathway. The attention has been focused on the analysis of the necroptosis pathway that was already reported as possibly deregulated in a mouse model of GD[79]. Necroptosis is a programmed and regulated necrosis process described for the first time almost 10 years ago[80], it represents a cellular response to environmental stress that can be induced by inflammation, chemical and mechanical injury or infection[81]. Essential mediators of this pathway are three receptor-interacting protein kinases (RIPKs): RIPK1, RIPK3 and MLKL, while the activation signal is probably mediated by the TNF- receptor system.

To test necroptosis activation in our GD model, RNA was extracted from cells both at iPSC level and after 15 and 19 days of macrophage differentiation and the expression levels of the three main pathway effectors have been analysed. While the mRNA levels of RIPK1 were not significantly different between the CNTR and GD lines, the expression levels of RIPK3 and MLKL were both strongly higher in the GD-1 line if compared with the CNTR, suggesting that necroptosis is highly activated when the GCase enzyme is not structurally and functionally present into the cell (Figure 8).

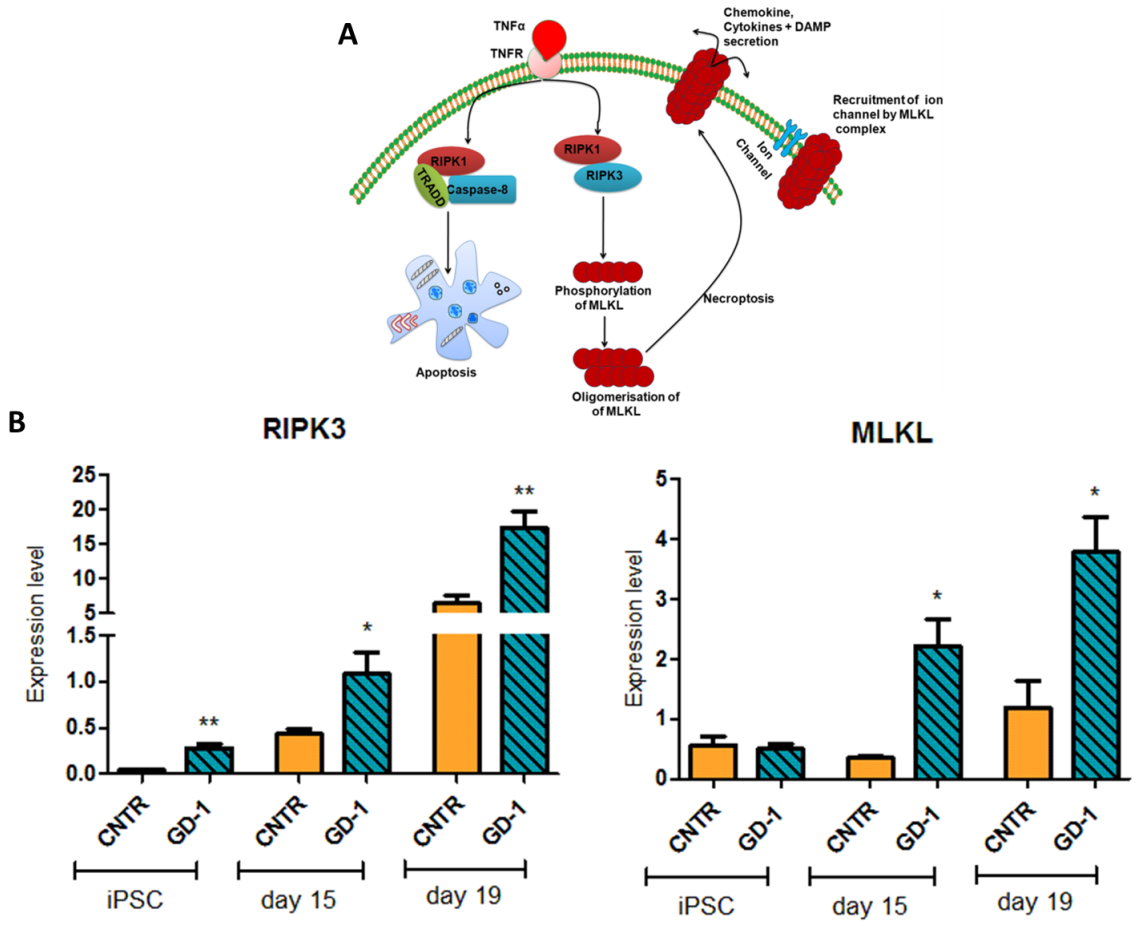


Figure 8: **Necroptosis is hyper-activated in the GD cell.** A) Schematic overview of the necroptosis pathway main effectors and their interactions (modified from Dhuriya et al, 2018[82]). B) Expression levels of RIPK3 and MLKL in CNTR and GD-1 lines at different differentiation stages. Statistical significance is indicated as p-value (Student's t-test), * $p<0.05$, ** $p<0.005$, n=3.

## 4.5 Gene correction of *GBA1* mutations through a ZFN strategy

The comparison of mutated lines with the isogenic gene corrected counterparts represents the best approach to explore common pathways evoked or disrupted by a pathogenic mutation. In order to have a more reliable comparison system, a ZFN strategy already developed and published by the Deleidi group of the university of Tübingen[70], has been exploited to try to gene correct the two reprogrammed patient lines (Figure 9A).

As already reported, the GD-1 patient presented a compound heterozygous condition for the two most common *GBA1* mutations: N370S (located on exon 9) and L444P (on exon 10). Cells have been nucleofected with ZFN designed to introduce a double strand break between exon 9 and 10 and the donor plasmid. After the antibiotic selection only three resistant colonies have been isolated, and just one presented at cDNA level the correction of the L444P mutation on exon 10, while N370S was still present into the genome, suggesting that the recombination occurred only in one allele.

The second patient (GD-2) carrying the N370S homozygous condition, was instead efficiently corrected in the mutation site with three different clones showing the wild type condition in both alleles at cDNA level (Figure 9B).

A third iPSC line (GD-3) derived from a homozygous L444P GD patient, already reprogrammed, gene corrected and characterized in the laboratory of Prof Deleidi, was included in the study considering the severe genotype, generally linked to neuronopathic manifestations.

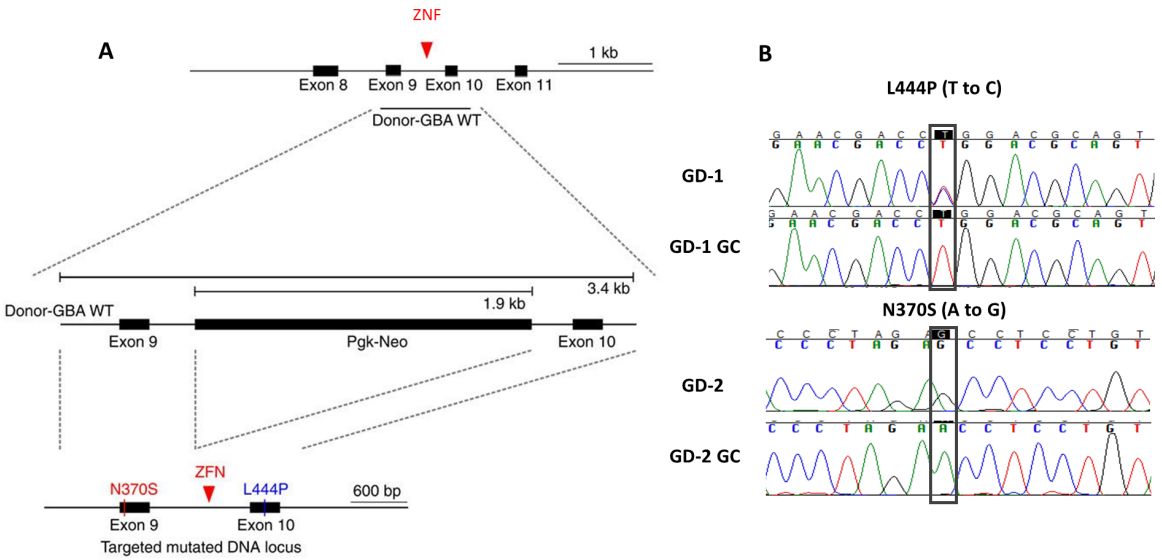


Figure 9: **Gene correction of the *GBA1* gene.** A) Schematic representation of the gene correction strategy taking advantage of ZFN to correct N370S and L444P mutations (from Schöndorf et al, 2014[70]. B) Electropherograms of the mutated and gene corrected lines in the mutation sites.

## 4.6 GD lines efficiently differentiate into midbrain dopaminergic neurons

Neuronopathic GD is a relatively rare condition among all the patient affected by the disease but is certainly the most severe and limiting form. Moreover, the biological mechanisms leading to the central nervous system involvement are still not clear and no effective therapeutic options are available. To try to better understand the molecular basis of this condition, GD-iPSC lines have been differentiated first towards the neural precursor, then towards the midbrain dopaminergic (mDA) neuronal fate.

Healthy donor-derived iPSC (CNTR) and the neuronopathic GD-3 lines underwent the differentiation protocol in parallel with the CBE treated (CNTR + CBE) and gene corrected (GD-3 GC) counterparts (Figure 10A). The first step of the differentiation protocol allowed to obtain homogeneous colonies of neuroepithelial cells, able to give rise to the three main neural populations: neurons, astrocytes and oligodendrocytes. At this differentiation stage cells are able to proliferate and maintain their lineage characteristics, they can be purified, expanded and used for experiments.

To obtain mature mDA neurons, NPC have been kept in culture for three further weeks with specific cytokines stimulation. At day 21 of neuronal differentiation cells showed a mature morphology and antigenic profile. The differentiation efficiency was proved by the expression of $\beta$3tubulin (neuronal marker) and TH (specific dopaminergic marker) (Figure 10B). The majority of both the GD and healthy cells expressed $\beta$3tubulin, while TH positive neurons are less then the half of the stained population in line with the protocol efficiency[75]. Mature cells have been fixed for immunostainings and collected for RNA and protein extraction.

## 4.7 GD iPSC-derived NPC show growth defects and an increased cell death rate

Considering that the previously obtained data on iPSC-derived monocyte/macrophage cells suggested that GCase functional deficit induces a growth defect, the growth potential of neural precursors have been analysed. GD-3 GC, GD-3, CNTR and CNTR+CBE NPC were seeded in standard culture condition and their number was evaluated after 3, 6, and 9 days in culture. GD lines displayed a strong reduction of the growth rate if compared with the not pathological counterpart, confirming the hypothesis that the enzyme deficit induces a decrease in cell proliferation and/or an increase in cell death also in neural lineage cells (Fig-

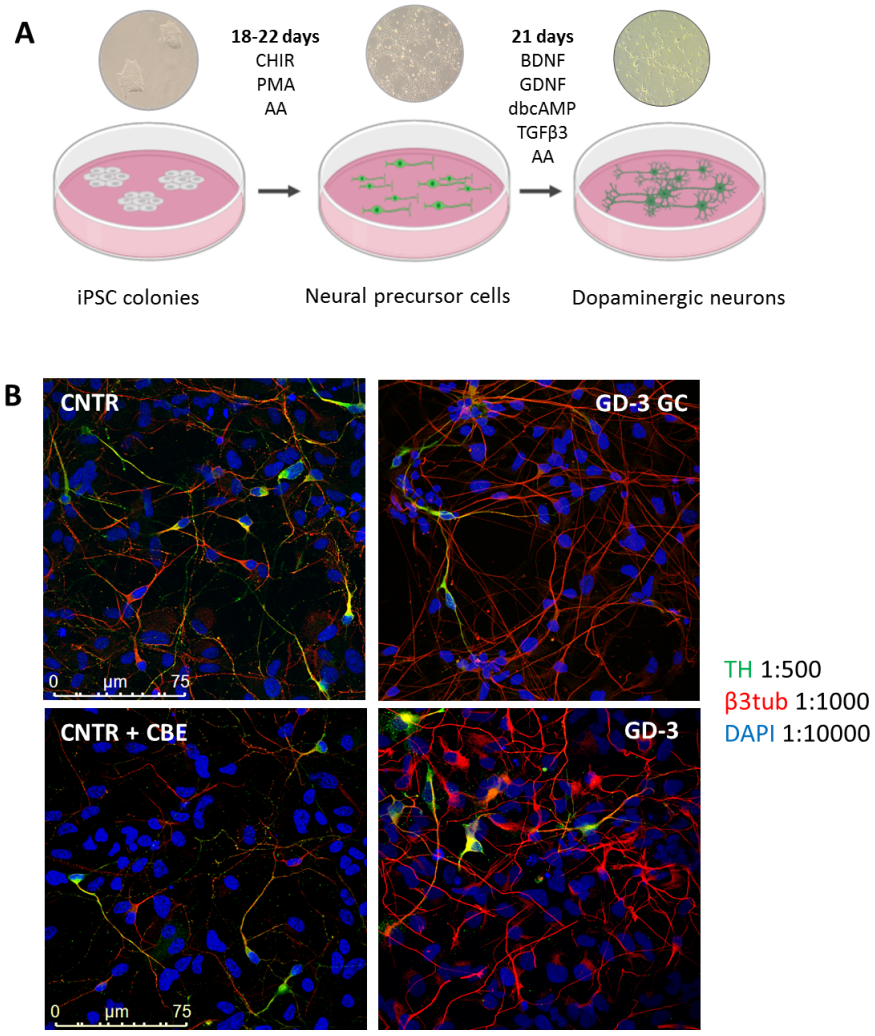


Figure 10: **mDA neurons differentiation of iPSC.** A) Main steps of the mDA neuronal differentiation protocol with the relative cytokines. B) Immunofluorescence pictures of terminally differentiated mDA neurons (24 days of differentiation from the NPC stage). Cells are stained for $\beta$3tubulin (red) and TH (green). Nuclei are counterstained with DAPI (blue). Magnification: 40X.

ure 11A).

To check if an upregulation of cell death pathways could occur in these cells, death and apoptosis rate were measured through flow cytometry. After 9 days in culture, NPC have been stained with the cell death marker, PI, and the apoptosis marker, annexin V. Interestingly, the overall cell death rate was higher in the GD lines, showing an increased percentage of PI positive cells if compared with the relative controls. The annexin V + cell population is not clearly identifiable in none of the lines, probably because cells have been analysed in too confluent culture condition where only late apoptotic cells are present (Figure 11B).

## 4.8 The Hippo pathway is hyperactivated in iPSC-derived neural GD cells

Since the necroptosis pathway main effectors resulted not highly expressed in the analysed lines at neuronal stage, we decided to focus our attention on another potentially interesting pathway that was already reported as deregulated in a GD Drosophila model by our group [83]. Hippo pathway is a highly structurally and functionally conserved molecular mechanism involved in the control of many cellular function, including development, tissue homeostasis, immunity, proliferation, tumorigenesis, apoptosis and cell death [84]. Hippo has gained a lot of attention for its tumor-suppressing task, but a considerable number of recently publications have highlighted the role of this pathway in inflaming neurodegeneration [85,86,87]. Considering that the hyper activation of the Hippo kinase core leads to the downregulation of proliferating and antiapoptotic genes (Figure 12A), its regulation can play a crucial role also in the neuronopathic GD condition.

For this purpose, the main Hippo pathway downstream targets, ANKHD1, CTGF and CYR61, expression levels have been analysed through qRT-PCR in the two couple of lines at both NPC and neuronal levels. All the targets appeared downregulated in the GD-3 NPC and mDA neurons compared with the gene corrected counterpart, suggesting a hyperactivation of the Hippo pathway core in the neural compartment (12B). The same trend was observed for two targets (CTGF and CYR61) also in the CNTR and CNTR+CBE comparison even if the difference was not statistically significant. Certainly, the GD patient-derived and GC couple is a more reliable model to study the pathway alterations in isogenic conditions, while the CBE treatment represents only an approximation of the physiological situation. CBE causes indeed just a functional deficit of the GCase enzyme but is not able to reproduce the complex cellular environment due to *GBA1* mutations.

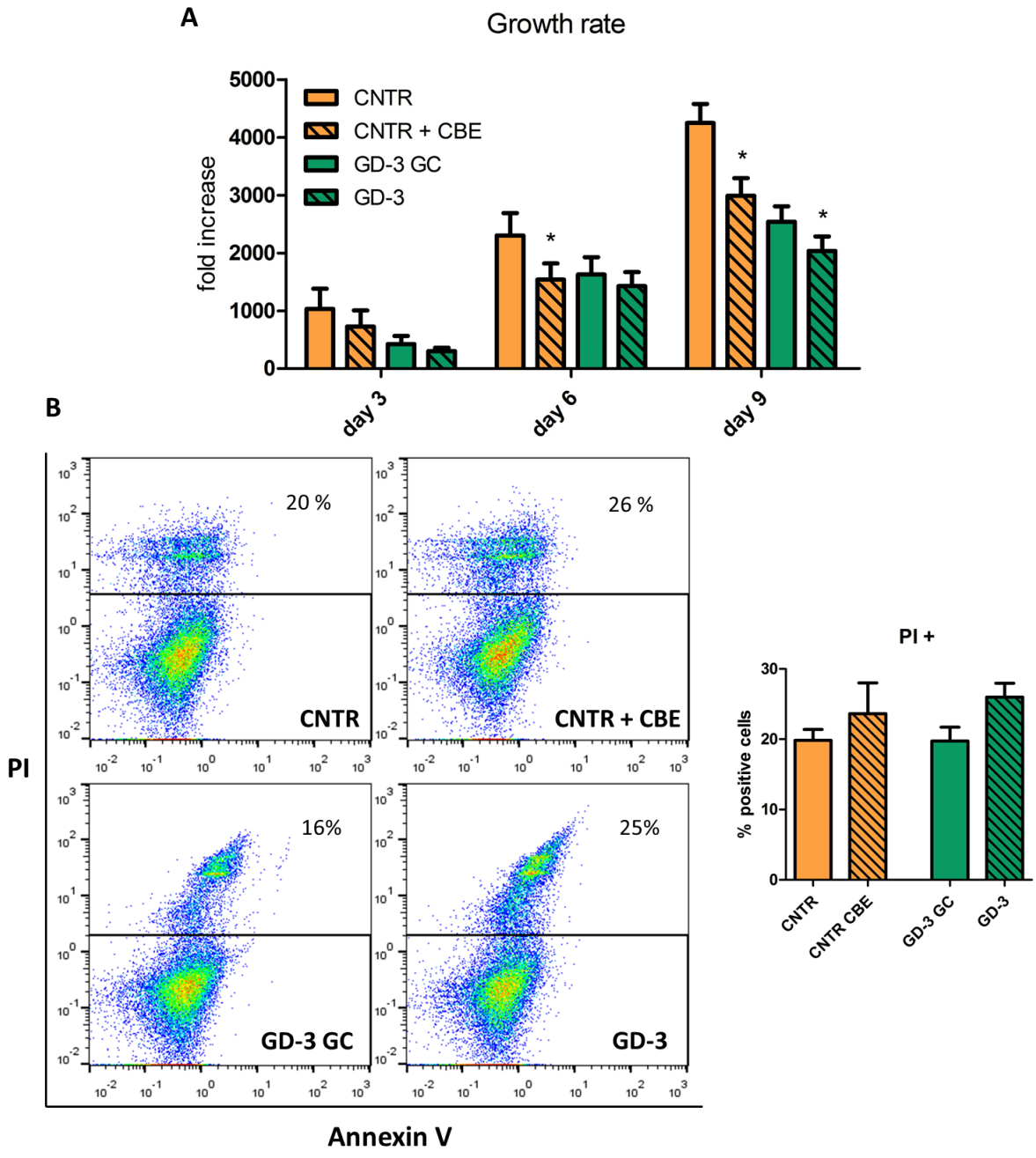


Figure 11: **GD neural precursor growth deficit.** A) Both GD-3 and CNTR+CBE show a significant growth defect after 9 days in culture. B) Flow cytometry evaluation of the four lines stained with annexin V (FITC) and PI and quantification of the PI marker positivity. Statistical significance is indicated as p-value (Student's t-test), * $p<0.05$, n=3.

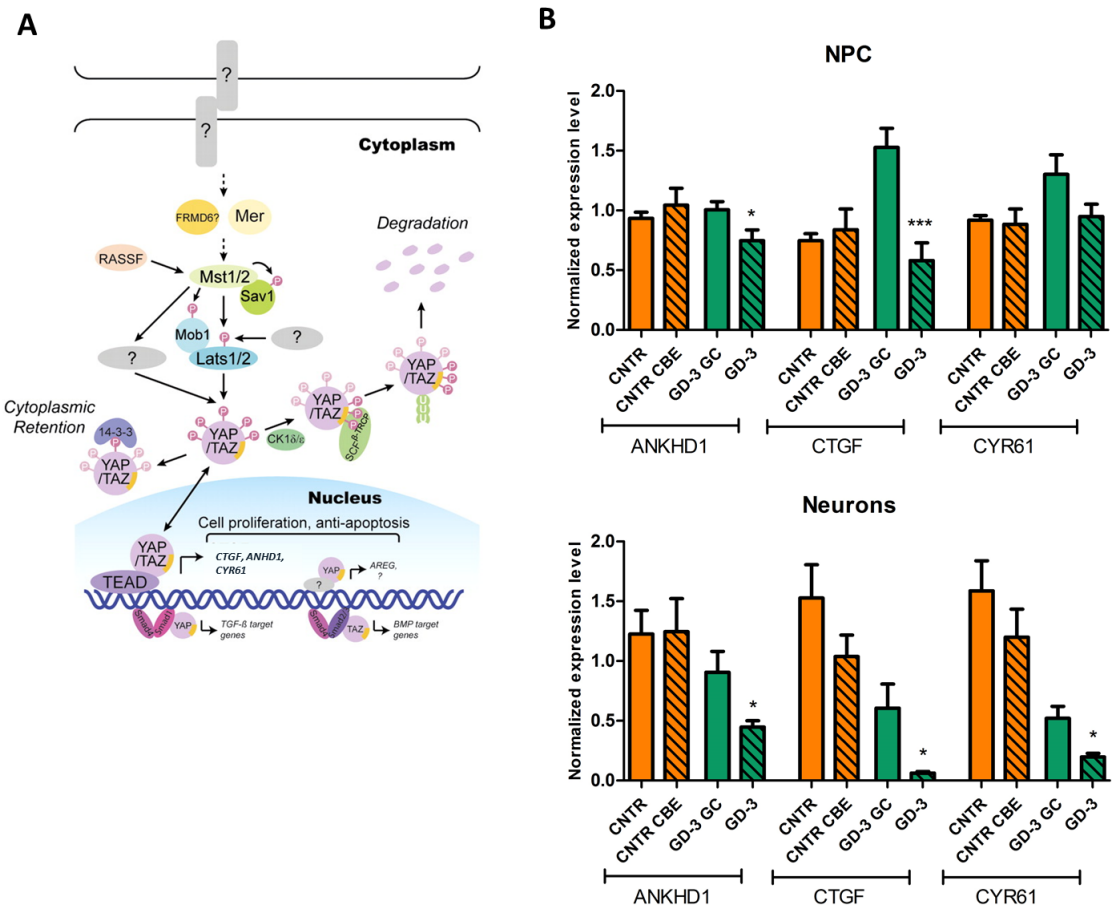


Figure 12: **YAP targets are transcriptionally downregulated in GD.** A) Scheme of the Hippo pathway main effectors in the human cell (modified from Zhao et al, 2010[88]. B) Hippo target genes are downregulated in iPSC-derived GD mDA neurons. Statistical significance is indicated as p-value (Student's t-test), * p<0.05, ***p<0.0005, n=3.

To unravel the pathway potential role the protein localization of YAP, the main Hippo effector, has been evaluated through immunofluorescence. YAP is a transcriptional factor able to reach the nucleus in the dephosphorylated form where it induces the transcription its wide number of downstream factors. When the Hippo pathway is active, YAP is phosphorylated and retained into the cytoplasm. Both NPC and mature neurons were fixed and stained with DAPI and a YAP specific antibody (Figure 13A). Immunofluorescence analysis of YAP subcellular localization revealed a significant decrease in the levels of YAP nuclear localization in GD-3 neural precursor and mDA neurons. Also CBE treated cell displayed a small reduction in the Hippo main effector nuclear localization (Figure 13B), suggesting that a hyper-Hippo condition can occur in iPSC-derived GD dopaminergic neurons.

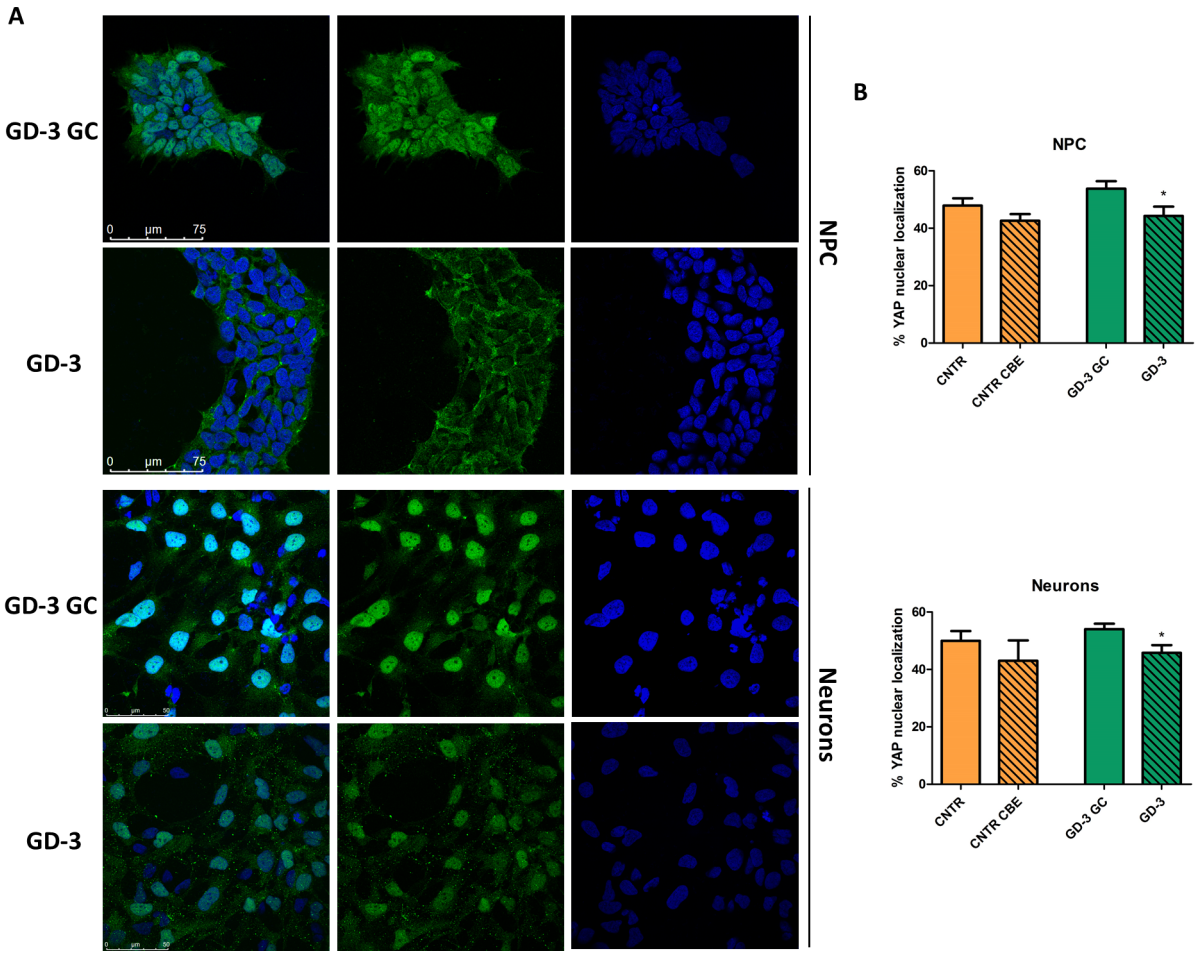


Figure 13: **YAP nuclear localization is reduced in GD iPSC-derived NPC and mDA neurons.** A) Representative pictures of YAP (green) cellular localization in the GD-3 and GD-3 GC NPC and neurons. Nuclei are counterstained with DAPI (blue). Magnification 63X. B) Quantification of the YAP nuclear localization in NPC and neurons performed with the Intensity Ratio Nuclei Cytoplasm Tool plug-in of the Fiji software. Statistical significance is indicated as p-value (Student's t-test), * $p<0.05$

# 5 Discussion

Despite the great improvements achieved in the last decades in the treatment and management of GD patients, different aspects of the pathology still remain problematic. Especially people affected by GD type 2 and 3 do not benefit from any therapeutic option and the only available interventions are focused on the reduction of the intensity and the progression of the symptomatology. ERT and SRT are instead a good option for patient without any neurological involvement, which are able to reverse the majority of the symptoms and prevent many complications. However, a delay in the diagnosis, that is not a rare event given the relatively non specific symptoms and the low frequency of the disease, can lead to irreversible morbidities[89,90].

Little is known about the molecular events leading to the different phenotypic manifestations and driving the wide symptomatological spectrum starting from a common mutational event in the GBA1 gene. Also the lack of correlation between the residual GCase activity and disease severity[91] opens to the hypothesis that exist other modifier genes underlying the phenotypic variation. A number of modulators of residual enzyme activity have been proposed as determinants of disease severity, including the lysosomal GCase activator saposin C[18], the lysosomal integral membrane protein type 2 (LIMP-2), identified as a sorting receptor for GCase[92] and levels of ER retention and ER-associated degradation in the proteasomes[93]. Genome wide association studies have been performed to identify new modifier in Ashkenazi Jewish patients with type 1 GD, homozygous for N370S mutation, where several single nucleotide polymophisms (SNPs) in linkage disequilibrium within the *CLN8* gene locus were associated with disease severity[94]. The same analysis was carried out also in GD mice injected with CBE displaying an highly phenotype variability in lifespan and symptoms and a big number of genes seemed to correlate with the disease severity, including genes controlling neuronal excitability (*Adk*, *Dpp10*, *Ctnnd2*, and *Grin2b*), endolysosomal biology (*Plekhf2* and *Atp6v1b2*) and brain development (*Fat4* and *Nf2*)[16]. However, the role of all these targets is the GD altered cell mechanisms is still not validated from a functional point of view.

A mechanistic approach more focused on the identification of whole signaling pathways alterations that could be involved in the modulation of GD proinflammatory condition, macrophage deficit and neuronal cell death are functional in better understanding the disease biology and patophysiology. To this end we devised an integrated approach aimed at identify-

ing key molecules and pathways that are responsible of the phenotypic features of visceral and neuronopathic GD by taking advantage of human iPSC models differentiated towards macrophages and neural cells. The technology of induced iPSC has a huge potential in the investigation of monogenic disease as GD, giving the opportunity to study specific mature cell populations recapitulating the human disease features. Moreover, the development of effective genome editing strategies gives the chance to perform experiment comparing patients iPSC lines with the isogenic gene corrected counterparts, representing the best tool to identify molecular pathways whose alteration is specifically driven by the disease pathological mutations. Our project was developed exploiting iPSC lines, derived from two type 1 and one type 3 GD patients and an healthy donor to dissect the key signaling pathways and pathogenetic mechanisms that foster GD progression in mature macrophages and neuronal cells. GD patients-derived iPSC have been gene corrected in the *GBA1* mutation site and fully characterized. From the analysis of cells differentiation potential was confirmed that GCase deficiency do not affect hematopoietic progenitors formation but GD lines tend to differentiate in a more efficient way towards the macrophage fate, expressing at an higher rate the specific lineage markers CD11b, CD14 and CD163. Interestingly, it was already reported in another iPSC-based study that GD hematopoietic progenitors demonstrated a marked lineage commitment, with increased myeloid differentiation and decreased erythroid differentiation and maturation, giving rise to adherent, macrophage-like cells, indicators of abnormal myelopoiesis[95]. The colony formation potential and the proliferation capacity of iPSC-derived monocyte/macrophages suggested that GD mature cells do not present a normal growth rate. The same deficit was evident also comparing the cell count of iPSC-derived GD neural precursors cell with controls lines, opening to the hypothesis that GCase enzyme deficit induces a growth defect in many cell types involved in the pathology. We decided to exploit an hypothesis-driven approach to identify signatures of selected pathways known or suspected to be involved in cell growth defect and inflammation in both monocyto/macrophage cells and in mDA neurons.

To this purpose, the expression levels of the three kinases of the necroptosis pathway (RIPK1, RIPK3 and MLKL) has been analysed in our lines at pluripotent state and at different time points during the macrophage differentiation. Necroptosis is a regulated form of necrotic cell death that has emerged as both an adaptive and pathogenic component of many human pathologies involving inflammatory processes[96]. A previously published study proved that the modulation of the RIPK3 protein improved neurological and systemic disease in a

mouse model of GD[79]. Interestingly, the two downstream necrosome complex components resulted hyperactivated in GD patient-derived cells confirming the idea that this pathway can play a role in triggering inflammation-related cell death processes in GD.

The second examined pathway, Hippo, gained a lot of attention in the last years for its many functions in restricting tissue growth in adults and modulating cell proliferation, differentiation, and migration in developing organs[97]. Deregulation of the Hippo pathway can lead to aberrant cell growth and neoplasia (hypo-Hippo) or to neurodegeneration (hyper-Hippo)[98]. The core of the Hippo pathway consists of a kinase cascade, transcription coactivators, and DNA-binding partners. YAP/TAZ are the main effectors of the Hippo signaling cascade[99] controlling the transcription of many different genes that are usually used as read-outs of the pathway activation. Our data demonstrate that the expression levels of three of the YAP transcriptional targets: ANKHD1, CTGF and CYR61 are downregulated in GD iPSC-derived NPC and mDA neurons and the hypothesis of a GD-related hyper Hippo condition was supported by the reduction of YAP nuclear localization in these cells. These results suggest that a hyper activation of the pathway can be implicated in the NPC decreased proliferation and in mature neurons degeneration, as reported in other neudegenerative disorders as Huntington's Disease[85], amyotrophic lateral sclerosis[100], retinal degeneration[101] and Alzheimer disease[86]. The wide number of interactions of the Hippo pathway with many cellular mechanisms make it a really interesting target; it was indeed reported to be involved in the control of inflammation[102], endoplasmic reticulum stress[103] and cell death[104], all mechanisms altered in GD. More precisely it is known to directly interact with some specific pathways impaired in GD models as mTOR[105], Wnt/$\beta$-catenin[106] and cathepsins activity[107]. Moreover, understanding of the pathological implications of Hippo in GD is particularly appealing also because many pharmacological modulators targeting Hippo are currently under evaluation for clinical applications[108].

The identification of two altered pathways in our iPSC-derived monocyte/macrophages and neurons proved the efficacy of this experimental model, that gives the opportunity to define gene expression patterns associated to *GBA1* loss or restoration in GD and isogenic gene corrected lines in the proper cell types. Furthermore, the understanding of which pathways are activated or repressed by *GBA1* loss of function and/or improper folding represents a valuable chance to fill the gap in the knowledge of modulator factors driving the different GD manifestations and to explore new strategies to approach the disease.

# References


1. P. Mistry, G. Lopez, R. Schiffman, N. Barton, N. Weinreb, and E. Sidransky, “Gaucher disease: Progress and ongoing challenges,” *Mol Genet Metab*, vol. 120, pp. 8–21, 2017.

2. L. Nalysnyk, P. Rotella, J. C. Simeone, A. Hamed, and N. Weinreb, “Gaucher disease epidemiology and natural history: a comprehensive review of the literature,” *Hematology*, vol. 22, pp. 65–73, 2017.

3. Y. Yamaguchi, N. Sasagasako, I. Goto, and T. Kobayashi, “The synthetic pathway for glucosylsphingosine in cultured fibroblasts,” *J Biochem*, vol. 116, pp. 704–710, 1994.

4. J. Stirnemann, N. Belmatoug, F. Camou, C. Serratrice, R. Froissart, C. Caillaud, T. Levade, L. Astudillo, J. Serratrice, A. Brassier, C. Rose, T. Billette de Villemeur, and M. Berger, “ A Review of Gaucher Disease Pathophysiology, Clinical Presentation and Treatments,” *Int J Mol Sci*, vol. 18, pp. 441–471, 2017.

5. R. E. Lee, “The fine structure of the cerebroside occurring in Gaucher’s disease,” *Proc Natl Acad Sci*, vol. 61, pp. 484–489, 1968.

6. P. Mistry, J. Liu, M. Yang, T. Nottoli, J. McGrath, D. Jain, K. Zhang, J. Keutzer, W. Chuang, W. Mehal, H. Zhao, A. Lin, and et al, “ Glucocerebrosidase gene-deficient mouse recapitulates Gaucher disease displaying cellular and molecular dysregulation beyond the macrophage,” *PNAS*, vol. 107, pp. 19473–19478, 2010.

7. K. Wong, E. Sidransky, A. Verma, T. Mixon, G. Sandberg, L. Wakefield, A. Morrison, A. Lwin, C. Colegial, J. Allman, and R. Schiffmann, “Neuropathology provides clues to the pathophysiology of Gaucher disease,” *Mol Genet Metab*, vol. 82, pp. 192–207, 2004.

8. E. Vitner, T. Farfel-Becker, R. Eilam, I. Biton, and A. Futerman, “Contribution of brain inflammation to neuronal cell death in neuronopathic forms of Gaucher’s disease,” *Brain*, vol. 135, pp. 1724–1735, 2012.

9. E. Orvisky, J. Park, M. LaMarca, E. Ginns, B. Martin, N. Tayebi, and E. Sidransky, “Glucosylsphingosine accumulation in tissues from patients with Gaucher disease: Correlation with phenotype and genotype,” *Mol Genet Metab*, vol. 76, pp. 262–270, 2002.

10. E. Lloyd-Evans, D. Pelled, C. Riebeling, and A. Futerman, “Lyso-glycosphingolipids mobilize calcium from brain microsomes via multiple mechanism,” *J Biochem*, vol. 375, pp. 561–565, 2003.

11. T. F. Barneveld RA, Keijzer W and et al, “Assignment of the gene coding for human beta-glucocerebrosidase to the region q21-q31 of chromosome 1 using monoclonal antibodies,” *Hum Genet*, vol. 64, pp. 227–231, 1983.

12. K. Hruska, M. LaMarca, R. Scott, and E. Sidransky, “Gaucher Disease: Mutation and PolymorphismSpectrum in the Glucocerebrosidase Gene (GBA),” *Hum Genet*, vol. 29, pp. 567–583, 2008.

13. L. Smith, S. Mullin, and A. Schapira, “Insights into the structural biology of Gaucher disease,” *Exp Neurol*, vol. 298, pp. 180–190, 2017.

14. G. Riboldi and A. Di Fonzo, “GBA, Gaucher Disease, and Parkinson’s Disease: From Genetic to Clinic to New Therapeutic Approaches,” *Cells*, vol. 8, p. E364, 2019.

15. D. Stone, N. Tayebi, E. Orvisky, B. Stubblefield, V. Madike, and E. Sidransky, “Glucocerebrosidase gene mutations in patients with type 2 Gaucher disease,” *Hum Mutat*, vol. 15, pp. 181–188, 2000.

16. A. Klein, N. Ferreira, S. Ben-Dor, J. Duan, J. Hardy, T. Cox, A. Merrill, and A. Futerman, “Identification of Modifier Genes in a Mouse Model of Gaucher Disease,” *Cell Reports*, vol. 16, pp. 2546–2553, 2016.

17. A. Velayati, J. De Paolo, N. Gupta, J. Choi, N. Moaven, W. Westbroek, O. Goker-Alpan, E. Goldin, B. Stubblefield, E. Kolodny, N. Tayebi, and E. Sidransky, “A mutation in SCARB2 is a modifier in Gaucher disease,” *Hum Mutat*, vol. 32, pp. 1232–1238, 2011.

18. R. Tamargo, A. Velayati, E. Goldin, and E. Sidransky, “The role of saposin C in Gaucher disease,” *Mol Genet Metab*, vol. 106, pp. 257–263, 2012.

19. A. Zimran, G. Altarescu, B. Rudensky, A. Abrahamov, and D. Elstein, “Survey of hematological aspects of Gaucher disease,” *Hematology*, vol. 10, pp. 151–156, 2005.

20. H. Baris, I. Cohen, and P. Mistry, “Gaucher Disease: The Metabolic Defect, Pathophysiology, Phenotypes And Natural History,” *Pediatr Endocrinol Rev*, vol. 12, pp. 72–81, 2014.

21. B. Rosenbloom, M. Balwani, J. Bronstein, E. Kolodny, S. Sathe, A. Gwosdow, J. Taylor, J. Cole, A. Zimran, and N. Weinreb, “The incidence of Parkinsonism in patients with type 1 Gaucher disease: data from the ICGG Gaucher registry,” *Blood Cells Mol Dis*, vol. 46, pp. 95–102, 2011.

22. K. Weiss, A. Gonzalez, G. Lopez, L. Pedoeim, C. Groden, and E. Sidransky, “The Clinical Management of Type 2 Gaucher Disease,” *Mol Genet Metab*, vol. 114, pp. 110–122, 2015.

23. I. Schwartz, O. Göker-Alpan, P. Kishnani, A. Zimran, L. Renault, Z. Panahloo, P. Deegan, and G. S. group, “Characteristics of 26 patients with type 3 Gaucher disease: A descriptive analysis from the Gaucher Outcome Survey,” *Mol Genet Metab*, vol. 14, pp. 73–79, 2018.

24. G. Grabowski, A. Zimran, and H. Ida, “Gaucher disease types 1 and 3: Phenotypic characterization of large populations from the ICGG Gaucher Registry,” *Am J Hematol*, vol. 90, pp. S12–18, 2015.

25. E. Sidransky, “Gaucher disease: Complexity in a “simple” disorder,” *Mol Genet Metab*, vol. 83, pp. 6–15, 2004.

26. M. Di Rocco, G. Andria, F. Deodato, F. Giona, C. Micalizzi, and A. Pession, “Early diagnosis of Gaucher disease in pediatric patients: proposal for a diagnostic algorithm,” *Pediatr Blood Cancer*, vol. 61, pp. 1905–1909, 2014.

27. P. Mistry, M. Cappellini, E. Lukina, H. Özsan, S. Pascual, and et al, “A reappraisal of Gaucher disease - diagnosis and disease management algorithms,” *American journal of hematology*, vol. 86, pp. 110–115, 2011.

28. E. Neufeld, “Lysosomal storage diseases,” *Annu Rev Biochem*, vol. 60, pp. 257–280, 1991.

29. C. Hollak, S. Van Weely, M. Van Oers, and J. Aerts, “Marked elevation of plasma chitotriosidase activity. A novel hallmark of Gaucher disease,” *J Clin Invest*, vol. 93, pp. 1288–1292, 1994.

30. N. Dekker, L. Van Dussen, C. Hollak, H. Overkleeft, S. Scheij, K. Ghauharali, M. Van Breemen, M. Ferraz, J. Groener, M. Maas, F. Wijburg, D. Speijer, A. Tylki-Szymanska, P. Mistry, R. Boot, and J. Aerts, “Elevated plasma glucosylsphingosine in

Gaucher disease: relation to phenotype, storage cell markers, and therapeutic response," *Blood*, vol. 118, pp. 118–127, 2011.

31. G. Polo, A. Burlina, T. Kolamunnage, M. Zampieri, C. Dionisi-Vici, P. Strisciuglio, M. Zaninotto, M. Plebani, and A. Burlina, "Diagnosis of sphingolipidoses: a new simultaneous measurement of lysosphingolipids by LC-MS/MS," *Clin Chem Lab Med*, vol. 55, pp. 403–414, 2017.

32. N. Weinreb, J. Charrow, H. Andersson, and et al, "Effectiveness of enzyme replacement therapy in 1028 patients with type 1 Gaucher disease after 2 to 5 years of treatment: a report from the Gaucher Registry," *Am J Med*, vol. 113, pp. 112–119, 2002.

33. R. Wenstrup, K. Kacena, and P. Kaplan, "Effect of enzyme replacement therapy with imiglucerase on BMD in type 1 Gaucher disease," *J Bone Miner Res*, vol. 22, pp. 119–126, 2007.

34. R. Dwek, T. Butters, F. Platt, and N. Zitzmann, "Targeting glycosylation as a therapeutic approach," *Nat Rev Drug Discov*, vol. 1, pp. 65–75, 2002.

35. E. Sidransky, D. Arkadir, P. Bauer, T. Dinur, G. Lopez, A. Rolfs, and A. Zimran, "Substrate reduction therapy for GBA1-associated Parkinsonism: Are we betting on the wrong mouse?," *Mov Disord*, vol. 35, pp. 228–230, 2020.

36. M. Coutinho, J. Santos, and S. Alves, "Less Is More: Substrate Reduction Therapy for Lysosomal Storage Disorders," *Int J Mol Sci*, vol. 17, p. 7, 2016.

37. D. Thirumal Kumar, S. Iyer, J. Christy, R. Siva, I. Tayubi, C. George Priya Doss, and H. Zayed, "A comparative computational approach toward pharmacological chaperones (NN-DNJ and ambroxol) on N370S and L444P mutations causing Gaucher's disease," *Adv Protein Chem Struct Biol*, vol. 114, pp. 315–339, 2019.

38. T. Han, R. Sam, and E. Sidransky, "Small Molecule Chaperones for the Treatment of Gaucher Disease and GBA1-Associated Parkinson Disease," *Front Cell Dev Biol*, vol. 8, p. 271, 2020.

39. H. Andersson, P. Kaplan, K. Kacena, and et al, "Eight year clinical outcomes of long term enzyme replacement therapy for 884 children with Gaucher disease type 1," *Pediatrics*, vol. 122, pp. 1182–1190, 2008.

40. J. Kanfer, G. Legler, J. Sullivan, S. Raghavan, and R. Mumford, “The Gaucher mouse,” *Biochem Biophys Res Commun*, vol. 67, pp. 85–90, 1975.

41. T. Farfel-Becker, E. Vitner, and A. Futerman, “Animal models for Gaucher disease research,” *Dis Model Mech*, vol. 6, pp. 746–752, 2011.

42. V. Tybulewicz, M. Tremblay, M. La Marca, R. Willemsen, B. Stubblefield, S. Winfield, B. Zablocka, E. Sidransky, B. Martin, and S. Huang, “Animal model of Gaucher’s disease from targeted disruption of the mouse glucocerebrosidase gene,” *Nature*, vol. 357, pp. 407–410, 1992.

43. R. Willemsen, V. Tybulewicz, E. Sidransky, W. Eliason, B. Martin, M. LaMarca, A. Reuser, M. Tremblay, H. Westphal, and R. Mulligan, “A biochemical and ultrastructural evaluation of the type 2 Gaucher mouse,” *Mol Chem Neuropathol*, vol. 24, pp. 179–192, 1995.

44. Y. Liu, K. Suzuki, J. Reed, A. Grinberg, H. Westphal, A. Hoffmann, T. Doring, K. Sandhoff, and R. Proia, “Mice with type 2 and 3 Gaucher disease point mutations generated by a single insertion mutagenesis procedure,” *Proc Natl Acad Sci*, vol. 95, pp. 2503–2508, 1998.

45. Y. Xu, R. Reboulet, B. Quinn, J. Huelsken, D. Witte, and G. Grabowski, “Dependence of reversibility and progression of mouse neuronopathic Gaucher disease on acid beta-glucosidase residual activity levels,” *Mol Genet Metab*, vol. 94, pp. 190–203, 2008.

46. I. Enquist, E. Nilsson, A. Ooka, J. Mansson, K. Olsson, M. Ehinger, R. Brady, J. Richter, and S. Karlsson, “Effective cell and gene therapy in a murine model of Gaucher disease,” *Proc Natl Acad Sci*, vol. 103, pp. 13819–13824, 2006.

47. I. Enquist, C. Bianco, A. Ooka, E. Nilsson, J. Mansson, M. Ehinger, J. Richter, R. Brady, D. Kirik, and S. Karlsson, “Murine models of acute neuronopathic Gaucher disease,” *Proc Natl Acad Sci*, vol. 104, pp. 17483–17488, 2007.

48. G. Maor, S. Rencus-Lazar, M. Filocamo, H. Steller, D. Segal, and M. Horowitz, “Unfolded protein response in Gaucher disease: from human to Drosophila,” *Orphanet J Rare Dis*, vol. 8, p. 140, 2013.

49. K. Kinghorn, S. Grönke, J. Castillo-Quan, N. Woodling, L. Li, E. Sirka, M. Gegg, K. Mills, J. Hardy, I. Bjedov, and L. Partridge, “A Drosophila Model of Neuronopathic Gaucher

Disease Demonstrates Lysosomal-Autophagic Defects and Altered mTOR Signalling and Is Functionally Rescued by Rapamycin," *J Neurosci*, vol. 46, pp. 11654–11670, 2016.

50. M. Suzuki, N. Fujikake, T. Takeuchi, A. Kohyama-Koganeya, K. Nakajima, Y. Hirabayashi, K. Wada, and Y. Nagai, "Glucocerebrosidase deficiency accelerates the accumulation of proteinase K-resistant -synuclein and aggravates neurodegeneration in a Drosophila model of Parkinson's disease," *J Neurosci*, vol. 23, pp. 6675–6686, 2015.

51. O. Cabasso, S. Paul, O. Dorot, G. Maor, O. Krivoruk, M. Pasmanik-Chor, M. Mirzaian, M. Ferraz, J. Aerts, and M. Horowitz, "Drosophila melanogaster Mutated in its GBA1b Ortholog Recapitulates Neuronopathic Gaucher Disease," *J Clin Med*, vol. 9, p. 1420, 2019.

52. M. Artola, C. Kuo, L. Lelieveld, R. Rowland, G. Van der Marel, J. Codée, R. Boot, G. Davies, J. Aerts, and H. Overkleeft, "Functionalized Cyclophellitols Are Selective Glucocerebrosidase Inhibitors and Induce a Bona Fide Neuropathic Gaucher Model in Zebrafish," *J Am Chem Soc*, vol. 141, pp. 4214–4218, 2019.

53. I. Zancan, S. Bellesso, R. Costa, M. Salvalaio, M. Stroppiano, C. Hammond, F. Argenton, M. Filocamo, and E. Moro, "Glucocerebrosidase deficiency in zebrafish affects primary bone ossification through increased oxidative stress and reduced Wnt/-catenin signaling," *Hum Mol Genet*, vol. 24, pp. 1280–1294, 2014.

54. M. Keatinge, H. Bui, A. Menke, Y. Chen, A. Sokol, Q. Bai, F. Ellett, M. Da Costa, D. Burke, M. Gegg, L. Trollope, T. Payne, A. McTighe, H. Mortiboys, S. de Jager, H. Nuthall, M. Kuo, A. Fleming, A. Schapira, S. Renshaw, J. Highley, A. Chacinska, P. Panula, E. Burton, M. O'Neill, and O. Bandmann, "Glucocerebrosidase 1 deficient Danio rerio mirror key pathological aspects of human Gaucher disease and provide evidence of early microglial activation preceding alpha-synuclein-independent neuronal cell death," *Hum Mol Genet*, vol. 24, pp. 6640–6652, 2015.

55. L. Lelieveld, M. Mirzaian, C. Kuo, M. Artola, M. Ferraz, R. Peter, H. Akiyama, P. Greimel, R. Van den Berg, H. Overkleeft, R. Boot, A. Meijer, and J. Aerts, "Role of -glucosidase 2 in aberrant glycosphingolipid metabolism: model of glucocerebrosidase deficiency in zebrafish," *J Lipid Res*, vol. 60, pp. 851–1867, 2019.

56. K. Takahashi and S. Yamanaka, “Induction of pluripotent stem cells from mouse embryonic and adult fibroblast cultures by defined factors,” *Cell*, vol. 126, pp. 663–676, 2006.

57. M. Doss and A. Sachinidis, “Current Challenges of iPSC-Based Disease Modeling and Therapeutic Implications,” *Cells*, vol. 8, p. 403, 2019.

58. C. Lee, R. Bendriem, W. Wu, and R. Shen, “3D brain Organoids derived from pluripotent stem cells: promising experimental models for brain development and neurodegenerative disorders,” *J Biomed Sci*, vol. 24, p. 59, 2017.

59. N. Gupta, E. Dilmen, and R. Morizane, “3D kidney organoids for bench-to-bedside translation,” *J Mol Med*, 2020.

60. M. Crespo, E. Vilar, S. Tsai, K. Chang, S. Amin, T. Srinivasan, T. Zhang, N. Pipalia, H. Chen, M. Witherspoon, M. Gordillo, J. Xiang, F. Maxfield, S. Lipkin, T. Evans, and S. Chen, “Colonic organoids derived from human induced pluripotent stem cells for modeling colorectal cancer and drug testing,” *Nat Med*, vol. 23, pp. 878–884, 2017.

61. H. Koike, K. Iwasawa, R. Ouchi, M. Maezawa, K. Giesbrecht, N. Saiki, A. Ferguson, M. Kimura, W. Thompson, J. Wells, A. Zorn, and T. Takebe, “Modelling human hepato-biliary-pancreatic organogenesis from the foregut-midgut boundary,” *Nature*, vol. 574, pp. 112–116, 2019.

62. D. Borger, B. McMahon, T. Roshan Lal, J. Serra-Vinardell, E. Aflaki, and E. Sidransky, “Induced pluripotent stem cell models of lysosomal storage disorders,” *Dis Model Mech*, vol. 10, pp. 691–704, 2017.

63. J. Kido, K. Nakamura, and T. Era, “Role of induced pluripotent stem cells in lysosomal storage diseases,” *Mol Cell Neurosci*, vol. 108, 2020.

64. L. Panicker, D. Miller, T. Park, B. Patel, J. Azevedo, O. Awad, M. Masood, T. Veenstra, E. Goldin, B. Stubblefield, N. Tayebi, S. Polumuri, S. Vogel, E. Sidransky, E. Zambidis, and R. Feldman, “Induced pluripotent stem cell model recapitulates pathologic hallmarks of Gaucher disease,” *Proc Natl Acad Sci*, vol. 109, pp. 18054–18059, 2012.

65. L. Panicker, D. Miller, O. Awad, V. Bose, Y. Lun, T. Park, E. Zambidis, J. Sgambato, and R. Feldman, “Gaucher iPSC-derived macrophages produce elevated levels of inflam-

matory mediators and serve as a new platform for therapeutic development," *Stem Cells*, vol. 32, pp. 2338–2349, 2014.

66. O. Awad, C. Sarkar, L. Panicker, D. Miller, X. Zeng, J. Sgambato, M. Lipinski, and R. Feldman, "Altered TFEB-mediated lysosomal biogenesis in Gaucher disease iPSC-derived neuronal cells," *Hum Mol Genet*, vol. 24, pp. 5775–5788, 2015.

67. Y. Sun, J. Florer, C. Mayhew, Z. Jia, Z. Zhao, K. Xu, H. Ran, B. Liou, W. Zhang, K. Setchell, J. Gu, and G. Grabowski, "Properties of neurons derived from induced pluripotent stem cells of Gaucher disease type 2 patient fibroblasts: potential role in neuropathology," *PLoS One*, vol. 10, 2015.

68. E. Aflaki, D. Borger, N. Moaven, B. Stubblefield, S. Rogers, S. Patnaik, F. Schoenen, W. Westbroek, W. Zheng, P. Sullivan, H. Fujiwara, R. Sidhu, Z. Khaliq, G. Lopez, D. Goldstein, D. Ory, J. Marugan, and E. Sidransky, "A New Glucocerebrosidase Chaperone Reduces -Synuclein and Glycolipid Levels in iPSC-Derived Dopaminergic Neurons from Patients with Gaucher Disease and Parkinsonism," *J Neurosci*, vol. 36, pp. 7441–7452, 2016.

69. L. Panicker, M. Srikanth, T. Castro-Gomes, D. Miller, N. Andrews, and R. Feldman, "Gaucher disease iPSC-derived osteoblasts have developmental and lysosomal defects that impair bone matrix deposition," *Hum Mol Genet*, vol. 27, pp. 811–822, 2018.

70. D. Schöndorf, M. Aureli, F. McAllister, C. Hindley, F. Mayer, B. Schmid, S. Sardi, M. Valsecchi, S. Hoffmann, L. Schwarz, U. Hedrich, D. Berg, L. Shihabuddin, J. Hu, J. Pruszak, S. Gygi, S. Sonnino, T. Gasser, and M. Deleidi, " iPSC-derived neurons from GBA1-associated Parkinson's disease patients show autophagic defects and impaired calcium homeostasis," *Nat Commun*, vol. 5, p. 4028, 2014.

71. H. Fernandes, E. Hartfield, H. Christian, E. Emmanoulidou, Y. Zheng, H. Booth, H. Bogetofte, C. Lang, B. Ryan, S. Sardi, J. Badger, J. Vowles, S. Evetts, G. Tofaris, K. Vekrellis, K. Talbot, M. Hu, W. James, S. Cowley, and R. Wade-Martins, "ER Stress and Autophagic Perturbations Lead to Elevated Extracellular -Synuclein in GBA-N370S Parkinson's iPSC-Derived Dopamine Neurons," *Stem Cell Reports*, vol. 6, pp. 342–356, 2016.

72. C. Woodard, B. Campos, S. Kuo, and et al, “iPSC-derived dopamine neurons reveal differences between monozygotic twins discordant for Parkinson’s disease,” *Cell Rep*, vol. 9, pp. 1173–1182, 2014.

73. D. Santos and G. Tiscornia, “Induced Pluripotent Stem Cell Modeling of Gaucher’s Disease: What Have We Learned?,” *Int J Mol Sci*, vol. 18, 2017.

74. S. Chou, M. Byrska-Bishop, J. Tober, Y. Yao, D. Vandorn, J. Opalinska, and et al, “Trisomy 21-associated defects in human primitive hematopoiesis revealed through induced pluripotent stem cells,” *Proc Natl Acad Sci*, vol. 109, pp. 17573–17578, 2012.

75. P. Reinhardt, M. Glatza, K. Hemmer, and et al, “ Derivation and expansion using only small molecules of human neural progenitors for neurodegenerative disease modeling,” *PLoS One*, vol. 8, p. 11, 2013.

76. M. Pandey, T. Burrow, R. Rani, L. Martin, D. Witte, K. Setchell, M. Mckay, A. Magnusen, W. Zhang, B. Liou, J. Köhl, and G. Grabowski, “Complement drives glucosylceramide accumulation and tissue inflammation in Gaucher disease,” *Nature*, vol. 543, pp. 108–112, 2017.

77. Y. Xu, L. Jia, B. Quinn, M. Zamzow, K. Stringer, B. Aronow, Y. Sun, W. Zhang, K. Setchell, and G. Grabowski, “Global gene expression profile progression in Gaucher disease mouse models,” *BMC Genomics*, vol. 12, p. 20, 2011.

78. A. Thomas, A. Mehta, and D. Hughes, “Gaucher disease: haematological presentations and complications,” *Br J Haematol*, vol. 165, pp. 427–440, 2014.

79. E. Vitner, R. Salomon, T. Farfel-Becker, A. Meshcheriakova, M. Ali, A. Klein, F. Platt, T. Cox, and A. Futerman, “RIPK3 as a potential therapeutic target for Gaucher’s diseasey,” *Nat Med*, vol. 20, pp. 204–208, 2014.

80. J. Hitomi, D. Christofferson, A. Ng, J. Yao, A. Degterev, R. Xavier, and J. Yuan, “Identification of a Molecular Signaling Network that Regulates a Cellular Necrotic Cell Death Pathway Cell,” *Br J Haematol*, vol. 135, pp. 1311–1323, 2008.

81. M. Khoury, K. Gupta, S. Franco, and B. Liu, “Necroptosis in the Pathophysiology of Disease,” *Am J Pathol*, vol. 190, pp. 272–285, 2020.

82. Y. Dhuriya and D. Sharma, “Necroptosis: a regulated inflammatory mode of cell death,” *J Neuroinflammation*, vol. 15, p. 199, 2018.

83. A. Astolfi, S. Messelodi, D Strocchi, S. Bertuccio, A. Taddia, A. Pession, D. Grifoni, and A. Pession, “Hippo and necroptosis pathways are involved in cell growth defects in Gaucher disease,” *Molecular Genetics and Metabolism*, vol. 126, p. S25, 2019.

84. Z. Wu and K. Guan, “Hippo Signaling in Embryogenesis and Development,” *Trends Biochem Sci*, vol. 11, p. S0968, 2020.

85. K. Mueller, K. Glajch, M. Huizenga, R. Wilson, E. Granucci, A. Dios, A. Tousley, M. Iuliano, E. Weisman, M. La Quaglia, M. Di Figlia, K. Kegel-Gleason, K. Vakili, and G. Sadri-Vakili, “Hippo Signaling Pathway Dysregulation in Human Huntington’s Disease Brain and Neuronal Stem Cells,” *Sci Rep*, vol. 8, p. 11355, 2018.

86. M. Irwin, M. Tare, A. Singh, O. Puli, N. Gogia, M. Riccetti, P. Deshpande, M. Kango-Singh, and A. Singh, “A Positive Feedback Loop of Hippo- and c-Jun-Amino-Terminal Kinase Signaling Pathways Regulates Amyloid-Beta-Mediated Neurodegeneration,” *Front Cell Dev Biol*, vol. 8, p. 117, 2020.

87. M. Sahu and A. Mondal, “The emerging role of Hippo signaling in neurodegeneration,” *J Neurosci Res*, vol. 98, pp. 796–814, 2020.

88. B. Zhao, L. Li, Q. Lei, , and K. Guan, “The Hippo–YAP pathway in organ size control and tumorigenesis: an updated version,” *Genes and Development*, vol. 24, pp. 862–874, 2010.

89. A. Mehta, D. Kuter, S. Salek, and et al, “Presenting signs and patient co-variables in Gaucher disease: outcome of the Gaucher Earlier Diagnosis Consensus (GED-C) Delphi initiative,” *Intern Med J*, vol. 49, pp. 578–591, 2019.

90. P. Mistry, S. Sadan, R. Yang, J. Yee, and M. Yang, “Consequences of diagnostic delays in type 1 Gaucher disease: the need for greater awareness among hematologists oncologists and an opportunity for early diagnosis and intervention,” *Am J Hematol*, vol. 82, pp. 697–701, 2007.

91. O. Goker-Alpan, K. Hruska, E. Orvisky, P. Kishnani, B. Stubblefield, R. Schiffmann, and E. Sidransky, “Divergent phenotypes in Gaucher disease implicate the role of modifiers,” *Med Genet*, vol. 42, 2005.

92. J. Blanz, J. Groth, C. Zachos, C. Wehling, P. Saftig, and M. Schwake, “Disease-causing mutations within the lysosomal integral membrane protein type 2 (LIMP-2) reveal the nature of binding to its ligand beta-glucocerebrosidase,” *Hum Mol Genet*, vol. 19, pp. 563–572, 2010.

93. I. Ron and M. Horowitz, “ER retention and degradation as the molecular basis underlying Gaucher disease heterogeneity,” *Hum Mol Genet*, vol. 14, pp. 2387–2398, 2005.

94. C. Zhang, P. Stein, J. Liu, Z. Wang, R. Yang, J. Cho, P. Gregersen, J. Aerts, H. Zhao, G. Pastores, and P. Mistry, “Genome-wide association study of N370S homozygous Gaucher disease reveals the candidacy of CLN8 gene as a genetic modifier contributing to extreme phenotypic variation,” *Am J Hematol*, vol. 87, pp. 377–383, 2012.

95. J. Sgambato, T. Park, D. Miller, L. Panicker, E. Sidransky, Y. Lun, O. Awad, S. Bentzen, E. Zambidis, and R. Feldman, “Gaucher Disease-Induced Pluripotent Stem Cells Display Decreased Erythroid Potential and Aberrant Myelopoiesis,” *Stem Cells Transl Med*, vol. 4, pp. 878–886, 2015.

96. M. Choi, D. Price, S. Ryter, and A. Choi, “Necroptosis: a crucial pathogenic mediator of human disease,” *JCI Insight*, vol. 4, p. e128834, 2019.

97. Z. Meng, T. Moroishi, and K. Guan, “Mechanisms of Hippo pathway regulation,” *Genes Dev*, vol. 30, pp. 1–17, 2016.

98. C. Pfleger, “The Hippo Pathway: A Master Regulatory Network Important in Development and Dysregulated in Disease,” *Curr Top Dev Biol*, vol. 123, pp. 181–228, 2017.

99. S. Piccolo, S. Dupont, and M. Cordenonsi, “The biology of YAP/TAZ: hippo signaling and beyond,” *Physiol Rev*, vol. 94, pp. 1287–1312, 2014.

100. G. Sadri-Vakili, K. Mueller, E. Granucci, A. Dios, J. Berry, and K. Vakili, “Alterations in Hippo pathway signaling as a mechanism of neuronal death in Amyotrophic Lateral Sclerosis,” *Expert Opin Ther Pat*, vol. 90, p. 436, 2018.

101. H. Matsumoto, Y. Murakami, K. Kataoka, and et al, “Mammalian STE20-like kinase 2, not kinase 1, mediates photoreceptor cell death during retinal detachment,” *Cell Death Dis*, vol. 5, p. e1269, 2014.

102. Y. Zhou, T. Huang, J. Zhang, A. Cheng, J. Yu, W. Kang, and K. To, “Emerging roles of Hippo signaling in inflammation and YAP-driven tumor immunity,” *Cancer Lett*, vol. 426, pp. 73–79, 2018.

103. S. Hou, L. Wang, and G. Zhang, “Mitofusin-2 regulates inflammation-mediated mouse neuroblastoma N2a cells dysfunction and endoplasmic reticulum stress via the Yap-Hippo pathway,” *J Physiol Sci*, vol. 69, pp. 697–709, 2019.

104. E. Fallahi, N. O’Driscoll, and D. Matallanas, “The MST/Hippo Pathway and Cell Death: A Non-Canonical Affair,” *Genes (Basel)*, vol. 7, p. 28, 2016.

105. R. Brown, A. Voit, M. Srikanth, J. Thayer, T. Kingsbury, M. Jacobson, M. Lipinski, R. Feldman, and O. Awad, “mTOR hyperactivity mediates lysosomal dysfunction in Gaucher’s disease iPSC-neuronal cells,” *Dis Model Mech*, vol. 16, 2019.

106. R. Costa, S. Bellesso, S. Lualdi, R. Manzoli, V. Pistorio, M. Filocamo, and E. Moro, “A transcriptional and post-transcriptional dysregulation of Dishevelled 1 and 2 underlies the Wnt signaling impairment in type I Gaucher disease experimental models,” *Hum Mol Genet*, vol. 15, pp. 274–285, 2020.

107. E. Vitner, H. Dekel, H. Zigdon, T. Shachar, R. Farfel-Becker, T nad Eilam, S. Karlsson, and A. Futerman, “Altered expression and distribution of cathepsins in neuronopathic forms of Gaucher disease and in other sphingolipidoses,” *Hum Mol Genet*, vol. 19, pp. 3583–3590, 2010.

108. J. Crawford, S. Bronner, and J. Zbieg, “Hippo pathway inhibition by blocking the YAP/TAZ-TEAD interface: a patent review,” *Expert Opin Ther Pat*, vol. 28, pp. 867–873, 2018.